

ZU-TH 06/05
IFT-6/2005
FERMILAB-PUB-05-531-T
hep-ph/0512066

Electromagnetic Logarithms in $\bar{B} \rightarrow X_s \ell^+ \ell^-$

Tobias Huber¹, Enrico Lunghi^{1,2}, Mikołaj Misiak^{1,3} and Daniel Wyler¹

¹ *Institute for Theoretical Physics, University of Zurich,
Winterthurerstrasse 190, CH-8057, Zurich, Switzerland.*

² *Fermi National Accelerator Laboratory,
P.O. Box 500, Batavia, IL 60510, U.S.A.*

³ *Institute of Theoretical Physics, Warsaw University,
Hoża 69, PL-00-681 Warsaw, Poland.*

Abstract

The $\bar{B} \rightarrow X_s \ell^+ \ell^-$ decay rate is known at the next-to-next-to-leading order in QCD. It is proportional to $\alpha_{em}(\mu)^2$ and has a $\pm 4\%$ scale uncertainty before including the $\mathcal{O}(\alpha_{em} \ln(M_W^2/m_b^2))$ electromagnetic corrections. We evaluate these corrections and confirm the earlier findings of Bobeth *et al.*. Furthermore, we complete the calculation of logarithmically enhanced electromagnetic effects by including also QED corrections to the matrix elements of four-fermion operators. Such corrections contain a collinear logarithm $\ln(m_b^2/m_\ell^2)$ that survives integration over the low dilepton invariant mass region $1 \text{ GeV}^2 < m_{\ell\ell}^2 < 6 \text{ GeV}^2$ and enhances the integrated decay rate in this domain. For the low- $m_{\ell\ell}^2$ integrated branching ratio in the muonic case, we find $\mathcal{B}(B \rightarrow X_s \mu^+ \mu^-) = (1.59 \pm 0.11) \times 10^{-6}$, where the error includes the parametric and perturbative uncertainties only. For $\mathcal{B}(B \rightarrow X_s e^+ e^-)$, in the current BaBar and Belle setups, the logarithm of the lepton mass gets replaced by angular cut parameters and the integrated branching ratio for the electrons is expected to be close to that for the muons.

1 Introduction

The inclusive decay $\bar{B} \rightarrow X_s \ell^+ \ell^-$ with $\ell = e$ or μ is known to be a sensitive probe of new physics at the electroweak scale. Its branching ratio has been recently measured by both Belle [1] and BaBar [2]. In the low dilepton invariant mass region, $1 \text{ GeV}^2 < m_{\ell\ell}^2 < 6 \text{ GeV}^2$, the experimental results read

$$\mathcal{B}(B \rightarrow X_s \ell^+ \ell^-) = (1.493 \pm 0.504^{+0.411}_{-0.321}) \times 10^{-6} \quad (\text{Belle}), \quad (1)$$

$$\mathcal{B}(B \rightarrow X_s \ell^+ \ell^-) = (1.8 \pm 0.7 \pm 0.5) \times 10^{-6} \quad (\text{BaBar}). \quad (2)$$

This leads to a world average

$$\mathcal{B}(B \rightarrow X_s \ell^+ \ell^-) = (1.60 \pm 0.51) \times 10^{-6}. \quad (3)$$

Measurements for lower and higher values of $m_{\ell\ell}^2$ are available, too. However, for higher $m_{\ell\ell}^2$, non-perturbative effects of the J/Ψ , Ψ' and higher resonances are sizeable, and the theoretical predictions have larger uncertainties. On the other hand, for $m_{\ell\ell}^2 < 1 \text{ GeV}^2$, the branching ratio is determined largely by the contribution from almost real intermediate photons, and it contains essentially the same information on new physics as is already known from the $\bar{B} \rightarrow X_s \gamma$ measurements. Throughout this paper, we restrict ourselves to the dilepton mass region $m_{\ell^+ \ell^-}^2 \in [1, 6] \text{ GeV}^2$.

The experimental errors in the branching ratio are expected to be substantially reduced in the near future. On the theoretical side, the predictions are quite well under control because the inclusive hadronic $\bar{B} \rightarrow X_s \ell^+ \ell^-$ decay rate for low dilepton mass is well approximated by the perturbatively calculable partonic $b \rightarrow X_s^{\text{parton}} \ell^+ \ell^-$ decay rate. Thanks to the recent (practically) complete calculation [3–9] of the Next-to-Next-to-Leading Order (NNLO) QCD corrections, the perturbative uncertainties are now below 10%.

The branching ratio is proportional to $\alpha_{\text{em}}^2(\mu)$ whose scale dependence cannot be neglected. Indeed, at the leading order in QED, $\mathcal{B}(B \rightarrow X_s \ell^+ \ell^-)$ changes from $1.54 \cdot 10^{-6}$ to $1.65 \cdot 10^{-6}$ when the renormalization scale of α_{em} is changed from $\mu = \mathcal{O}(m_b)$ to $\mu = \mathcal{O}(M_W)$. This uncertainty is removed by calculating those QED corrections that are enhanced by large logarithms $\ln(M_H^2/M_L^2)$, where $M_H \sim M_W, m_t$ and $M_L \sim m_b, m_{\ell\ell}$.

In Ref. [9], the QED corrections to the Wilson coefficients were calculated, thereby giving most of the electromagnetic corrections that are enhanced by $\ln(M_H^2/M_L^2)$. As a result, the authors find a branching ratio of $1.56 \cdot 10^{-6}$, * which incidentally corresponds to setting $\alpha_{\text{em}}^2 = \alpha_{\text{em}}^2(\mu \sim m_b)$ at the leading order in QED. We have calculated and confirm the results of Ref. [9] for all the two-loop anomalous dimension matrices that determine the size of the $\ln(M_H^2/M_L^2)$ -enhanced electromagnetic corrections.

However, there are additional QED corrections that get enhanced by large logarithms, namely $\ln(m_b^2/m_{\ell\ell}^2)$. These corrections are the new result of the present paper. They originate from these parts of the QED bremsstrahlung corrections where the photon is collinear

*The number quoted by the authors of Ref. [9] and on which we agree is $1.57 \cdot 10^{-6}$. In the text we give the result obtained using the updated experimental inputs summarized in Table 1.

with one of the outgoing leptons. They disappear after integration over the whole available phase space but survive and remain numerically important when $m_{\ell\ell}^2$ is restricted to the region that we consider.

Such logarithmic corrections are found under the assumption that no collinear photons are included in the definition of the dilepton invariant mass. This turns out to be a very good approximation for the muons in the current BaBar and Belle setups [10]. In this case, the enhancement of the low- $m_{\ell\ell}^2$ integrated branching ratio by the collinear logarithms amounts to around 2%. The corresponding effect for the electrons would reach around 5%. However, in that case, the logarithm of the electron mass gets replaced by the BaBar and Belle angular cut parameters and the integrated branching ratio for the electrons is expected to be close to that for the muons. We shall describe this issue in more detail in Section 6. In the preceeding sections, our analytical and numerical results will correspond to the case of perfect separation of electrons and energetic collinear photons.

Before we come to the results and details of the calculation, some comments on its systematics are in order. Due to the different scales involved, the perturbative corrections come not only with increasing powers of some coupling constant, but also with increasing powers of the large logarithm $L = \ln(M_H^2/M_L^2)$. The perturbative calculation results in an expansion in the product of the coupling with L rather than in the coupling alone.

Because α_s is relatively large, all powers of $c_s = \alpha_s L$ must be resummed at a given order of the perturbative expansion, which is achieved using the renormalization group technology. Within this framework, all the logarithms L are absorbed into $c_s = \mathcal{O}(1)$. Consequently, each electromagnetic logarithm $\alpha_{em}L = c_s\alpha_{em}/\alpha_s$ of the conventional perturbative expansion gets replaced by $f(c_s)\alpha_{em}/\alpha_s$, where the function $f(c_s)$ is found by solving the renormalization group equations. Such a replacement of the electromagnetic logarithm is not a matter of convenience but an unavoidable consequence of resumming the QCD logarithms and not resumming the QED ones. Resummation of the QED logarithms would be technically more difficult and also unnecessary, because $\alpha_{em}L \ll 1$. Thus, the conventional expansion in α_s and α_{em} is replaced by an expansion in α_s and in $\kappa \equiv \alpha_{em}/\alpha_s$. Each order of this expansion is calculated exactly in c_s .

The amplitude of $B \rightarrow X_s \ell^+ \ell^-$ is proportional to α_{em} . The Leading Order (LO) contributions come from loops and are of order κ (the electromagnetic logarithm comes from a loop). Higher order terms that are proportional to $\kappa\alpha_s$ and $\kappa\alpha_s^2$ are conventionally called the NLO and NNLO QCD contributions, respectively. However, since $\kappa\alpha_s = \alpha_{em}$, the NLO contributions contain purely electroweak terms, too. Since these NLO terms are enhanced by $m_t^2/(M_W^2 \sin^2 \theta_W)$ while the LO terms are accidentally suppressed, the two contributions turn out to be very similar in size. An analogous effect occurs at order κ^2 : the terms of order $\kappa^2\alpha_s^1$ are larger than the $\kappa^2\alpha_s^0$ ones. For this reason, also high terms in the $\kappa^n\alpha_s^m$ -expansion remain numerically important.

The corrections to be considered here (and also in Ref [9]) are of order κ^2 and $\kappa^2\alpha_s$ in the decay amplitude. Contributions corresponding to $\kappa^2\alpha_s^2 \simeq \alpha_{em}^2$ in the amplitude will be included only if they are enhanced by $\ln(m_b^2/m_\ell^2)$ or by an additional factor of $m_t^2/(M_W^2 \sin^2 \theta_W)$.

Our article is organized as follows. In Section 2 we summarize the results for the branching

ratio and explain details of the $\kappa^n \alpha_s^m$ -expansion. The effective theory used for resummation of large QCD logarithms is introduced in Section 3 which is quite technical. It includes the list of the relevant operators, the matching conditions for the Wilson coefficients, the renormalization group equations and the Wilson coefficients at the low scale. Sections 4 and 5 contain a detailed description of the four-fermion operator matrix element calculation. In Section 6 we discuss the role of the angular cuts. Master formulae for the branching ratio are summarized in Section 7. Appendix A contains the loop functions that appear in the text. Some intermediate-step quantities for the evolution of Wilson coefficients are collected in Appendix B. Appendix C is devoted to describing techniques that we have used to calculate the QED matrix elements of quark-lepton operators.

2 Branching ratio and numerical results

In order to facilitate the reading of this rather technical paper, we give the final results first. The differential (with respect to $\hat{s} = m_{\ell\ell}^2/m_{b,\text{pole}}^2$) decay width of $\bar{B} \rightarrow X_s \ell^+ \ell^-$ can be expressed as follows:

$$\frac{d\Gamma(\bar{B} \rightarrow X_s \ell^+ \ell^-)}{d\hat{s}} = \frac{G_F^2 m_{b,\text{pole}}^5}{48\pi^3} |V_{ts}^* V_{tb}|^2 \Phi_{\ell\ell}(\hat{s}), \quad (4)$$

where the dimensionless function $\Phi_{\ell\ell}(\hat{s})$ is assumed to include both the perturbative and non-perturbative contributions.

In order to minimize the uncertainty stemming from $m_{b,\text{pole}}^5$ and the CKM angles, we normalize the rare decay rate to the measured semileptonic one. Furthermore, to avoid introduction of spurious uncertainties due to the perturbative $b \rightarrow X_c e \bar{\nu}$ phase-space factor, we follow the analyses of Refs. [9, 11] where

$$C = \left| \frac{V_{ub}}{V_{cb}} \right|^2 \frac{\Gamma(\bar{B} \rightarrow X_c e \bar{\nu})}{\Gamma(\bar{B} \rightarrow X_u e \bar{\nu})}, \quad (5)$$

was used instead. Consequently, our expression for the $\bar{B} \rightarrow X_s \ell^+ \ell^-$ branching ratio reads

$$\frac{d\mathcal{B}(\bar{B} \rightarrow X_s \ell^+ \ell^-)}{d\hat{s}} = \mathcal{B}(B \rightarrow X_c e \bar{\nu})_{\text{exp}} \left| \frac{V_{ts}^* V_{tb}}{V_{cb}} \right|^2 \frac{4}{C} \frac{\Phi_{\ell\ell}(\hat{s})}{\Phi_u}, \quad (6)$$

where $\Phi_u = 1 + \mathcal{O}(\alpha_s, \alpha_{em}, \Lambda^2/m_b^2)$ is defined by

$$\Gamma(B \rightarrow X_u e \bar{\nu}) = \frac{G_F^2 m_{b,\text{pole}}^5}{192\pi^3} |V_{ub}|^2 \Phi_u. \quad (7)$$

Our expressions for the ratio $\Phi_{\ell\ell}(\hat{s})/\Phi_u$ are summarized in Section 7. Both the perturbative and non-perturbative corrections to this ratio are much better behaved than for $\Phi_{\ell\ell}(\hat{s})$ and Φ_u separately. The factor $C = 0.58 \pm 0.01$ has been recently determined from a global analysis of the semileptonic data [12]. All the input parameters that we use in the numerical calculation are summarized in Table 1.

$\alpha_s(M_z) = 0.1182 \pm 0.0027$ [13]	$m_e = 0.51099892$ MeV
$\alpha_e(M_z) = 1/127.918$	$m_\mu = 105.658369$ MeV
$s_W^2 \equiv \sin^2 \theta_W = 0.2312$	$m_\tau = 1.77699$ GeV
$ V_{ts}^* V_{tb} / V_{cb} ^2 = 0.967 \pm 0.009$ [14]	$m_c(m_c) = (1.224 \pm 0.017 \pm 0.054)$ GeV [15]
$BR(B \rightarrow X_c e \bar{\nu})_{\text{exp}} = 0.1061 \pm 0.0017$ [16]	$m_b^{1S} = (4.68 \pm 0.03)$ GeV [12]
$M_Z = 91.1876$ GeV	$m_{t,\text{pole}} = (172.7 \pm 2.9)$ GeV [17]
$M_W = 80.426$ GeV	$m_B = 5.2794$ GeV
$\lambda_2 \simeq \frac{1}{4} (m_{B^*}^2 - m_B^2) \simeq 0.12$ GeV ²	$C = 0.58 \pm 0.01$ [12]

Table 1: Numerical inputs that we use in the phenomenological analysis. Unless explicitly specified, they are taken from PDG 2004 [18].

It should be stressed that the pole mass of the b quark that is present in the definition of \hat{s} and in several loop functions gets analytically converted to the so-called $1S$ -mass before any numerical evaluation of the branching ratio is performed. This way one avoids dealing with the renormalon ambiguities in the definition of the pole mass [19]. The formula that relates the pole mass to the $1S$ -mass can be found e.g. in section 4 of Ref. [20].

Let us explain the details of the α_s and κ expansion that we adopt for calculating our final numerical results. The $b \rightarrow s \ell^+ \ell^-$ decay amplitude has the following structure (up to an overall factor of G_F):

$$\begin{aligned} \mathcal{A} = & \kappa \left[\mathcal{A}_{LO} + \alpha_s \mathcal{A}_{NLO} + \alpha_s^2 \mathcal{A}_{NNLO} + \mathcal{O}(\alpha_s^3) \right] \\ & + \kappa^2 \left[\mathcal{A}_{LO}^{\text{em}} + \alpha_s \mathcal{A}_{NLO}^{\text{em}} + \alpha_s^2 \mathcal{A}_{NNLO}^{\text{em}} + \mathcal{O}(\alpha_s^3) \right] + \mathcal{O}(\kappa^3). \end{aligned} \quad (8)$$

As mentioned in the introduction, $\mathcal{A}_{LO} \sim \alpha_s \mathcal{A}_{NLO}$ and $\mathcal{A}_{LO}^{\text{em}} \sim \alpha_s \mathcal{A}_{NLO}^{\text{em}}$. All these terms are included in our calculation in a complete manner, together with the appropriate bremsstrahlung corrections. As far as \mathcal{A}_{NNLO} is concerned, we use the practically complete results of Refs. [3–9]; the only missing parts originate from the unknown two-loop matrix elements of the QCD-penguin operators whose Wilson coefficients are very small.

Among the contributions to $\mathcal{A}_{NNLO}^{\text{em}}$, we include only the terms which are either enhanced by an additional factor of $m_t^2/(M_W^2 \sin^2 \theta_W)$ (with respect to $\mathcal{A}_{NLO}^{\text{em}}$) [9] or contribute to the $\ln(m_b^2/m_\ell^2)$ -enhanced terms at the decay width level. The latter terms are calculated for the first time here. They are taken into account in a practically complete manner; the only missing part is proportional to the same tiny Wilson coefficient that is responsible for the smallness of \mathcal{A}_{LO} .

The perturbative expansion of the ratio $\Phi_{\ell\ell}(\hat{s})/\Phi_u$ has a similar structure to that of the

squared amplitude:

$$\begin{aligned}
\mathcal{A}^2 &= \kappa^2 \left[\mathcal{A}_{LO}^2 + \alpha_s 2\mathcal{A}_{LO}\mathcal{A}_{NLO} + \alpha_s^2 (\mathcal{A}_{NLO}^2 + 2\mathcal{A}_{LO}\mathcal{A}_{NNLO}) \right. \\
&\quad \left. + \alpha_s^3 2(\mathcal{A}_{NLO}\mathcal{A}_{NNLO} + \dots) + \mathcal{O}(\alpha_s^4) \right] \\
&+ \kappa^3 \left[2\mathcal{A}_{LO}\mathcal{A}_{LO}^{em} + \alpha_s 2(\mathcal{A}_{NLO}\mathcal{A}_{LO}^{em} + \mathcal{A}_{LO}\mathcal{A}_{NLO}^{em}) \right. \\
&\quad \left. + \alpha_s^2 2(\mathcal{A}_{NLO}\mathcal{A}_{NLO}^{em} + \mathcal{A}_{NNLO}\mathcal{A}_{LO}^{em} + \mathcal{A}_{LO}\mathcal{A}_{NNLO}^{em}) \right. \\
&\quad \left. + \alpha_s^3 2(\mathcal{A}_{NLO}\mathcal{A}_{NNLO}^{em} + \mathcal{A}_{NNLO}\mathcal{A}_{NLO}^{em} + \dots) + \mathcal{O}(\alpha_s^4) \right] \\
&+ \mathcal{O}(\kappa^4).
\end{aligned} \tag{9}$$

In our numerical calculation of $\Phi_{\ell\ell}(\hat{s})/\Phi_u$, we include all the terms that are written explicitly in the above equations. The dots at orders $\kappa^2\alpha_s^3$ and $\kappa^3\alpha_s^3$ stand for terms that are proportional to \mathcal{A}_{LO} and \mathcal{A}_{LO}^{em} and, consequently, can safely be neglected. In the numerical analysis we also include subleading $1/m_c$ and $1/m_b$ corrections [21–23] as well as finite bremsstrahlung effects [5].

Our results for the branching ratios integrated in the range $1 \text{ GeV}^2 < m_{\ell\ell}^2 < 6 \text{ GeV}^2$ read

$$\begin{aligned}
\mathcal{B}_{\mu\mu} &= \left[1.59 \pm 0.08_{\text{scale}} \pm 0.06_{m_t} \pm 0.024_{C,m_c} \pm 0.015_{m_b} \right. \\
&\quad \left. \pm 0.02_{\alpha_s(M_Z)} \pm 0.015_{\text{CKM}} \pm 0.026_{\text{BR}_{sl}} \right] \times 10^{-6} = (1.59 \pm 0.11) \times 10^{-6},
\end{aligned} \tag{10}$$

$$\begin{aligned}
\mathcal{B}_{ee} &= \left[1.64 \pm 0.08_{\text{scale}} \pm 0.06_{m_t} \pm 0.025_{C,m_c} \pm 0.015_{m_b} \right. \\
&\quad \left. \pm 0.02_{\alpha_s(M_Z)} \pm 0.015_{\text{CKM}} \pm 0.026_{\text{BR}_{sl}} \right] \times 10^{-6} = (1.64 \pm 0.11) \times 10^{-6}.
\end{aligned} \tag{11}$$

The central values are obtained for the matching scale $\mu_0 = 120 \text{ GeV}$ and the low-energy scale $\mu_b = 5 \text{ GeV}$. The uncertainty from missing higher order perturbative corrections have been estimated by increasing and decreasing the scales $\mu_{0,b}$ by factors of 2. Uncertainties induced by m_t , m_b , m_c , C , $\alpha_s(M_Z)$, the CKM angles and the semileptonic rate are obtained by varying the various inputs within the errors given in Table 1; we assume the errors on C and m_c to be fully correlated. The total error is obtained by adding the individual uncertainties in quadrature. The electron and muon channels receive different contributions because of the $\ln(m_b^2/m_\ell^2)$ present in the bremsstrahlung corrections. The difference gets reduced when the BaBar and Belle angular cuts are included (see Sec. 6).

We stress that the indicated uncertainties are only the parametric and perturbative ones. No additional uncertainty for the unknown subleading non-perturbative corrections has been included. In particular, we believe that the uncalculated order $\alpha_s(\mu_b) \frac{\Lambda_{QCD}}{m_{c,b}}$ non-perturbative corrections imply an additional uncertainty of around $\sim 5\%$ in the above formula. This issue deserves an independent study.

One should also keep in mind that all the effects of the intermediate ψ and ψ' contributions are assumed to be subtracted on the experimental side. This refers, in particular, to the decays $\psi \rightarrow X\ell^+\ell^-$ where low-mass dilepton pairs can be produced. All such decays of the ψ with branching ratios down to 10^{-5} may be relevant. To our knowledge, only $X = \gamma$ has been considered so far in the experimental analyses.

NLO ($\alpha_{em}(\mu_0)$)	1.81×10^{-6}	NLO ($\alpha_{em}(\mu_b)$)	1.68×10^{-6}
NNLO ($\alpha_{em}(\mu_0)$)	1.65×10^{-6}	NNLO ($\alpha_{em}(\mu_b)$)	1.54×10^{-6}
QED (only WC's)	1.56×10^{-6}		
QED (muons)	1.59×10^{-6}	QED (electrons)	1.64×10^{-6}

Table 2: Anatomy of QCD and QED corrections.

The overall uncertainties in Eqs. (10) and (11) are somewhat smaller than in Eq. (27) of Ref. [9]. This is mainly due to the improved experimental value of m_t as well as to our use of m_b^{1S} rather than $m_{b,\text{pole}}$. The latter opportunity was already suggested in Ref. [9].

In Table 2, we show the partial results that we obtain by adding sequentially all the known QCD and QED corrections. The rows denoted by “NLO” and “NNLO” refer to the leading order in QED. The row “QED (only WC's)” contains only those QED corrections that stem from the Wilson coefficients. The row “QED” includes all the electromagnetic corrections (that are different for electrons and muons, as in Eqs. (10) and (11)).

A numerical formula that gives the branching ratio for non-SM values of the high-scale Wilson coefficients of the operators P_7 , P_8 , P_9 and P_{10} (see Section 3) reads

$$\begin{aligned} \mathcal{B}_{\mu\mu} = & \left[2.1913 - 0.001655 \mathcal{I}(R_{10}) + 0.0005 \mathcal{I}(R_{10}R_8^*) + 0.0535 \mathcal{I}(R_7) + 0.02266 \mathcal{I}(R_7R_8^*) \right. \\ & + 0.00496 \mathcal{I}(R_7R_9^*) + 0.00513 \mathcal{I}(R_8) + 0.0261 \mathcal{I}(R_8R_9^*) - 0.0118 \mathcal{I}(R_9) \\ & - 0.5426 \mathcal{R}(R_{10}) + 0.0281 \mathcal{R}(R_7) + 0.0153 \mathcal{R}(R_7R_{10}^*) + 0.06859 \mathcal{R}(R_7R_8^*) \\ & - 0.8554 \mathcal{R}(R_7R_9^*) - 0.00866 \mathcal{R}(R_8) + 0.00185 \mathcal{R}(R_8R_{10}^*) - 0.0981 \mathcal{R}(R_8R_9^*) \\ & + 2.7008 \mathcal{R}(R_9) - 0.10705 \mathcal{R}(R_9R_{10}^*) + 10.7687 |R_{10}|^2 + 0.2889 |R_7|^2 \\ & \left. + 0.00381 |R_8|^2 + 1.4892 |R_9|^2 \right] \times 10^{-7}, \end{aligned} \quad (12)$$

$$\begin{aligned} \mathcal{B}_{ee} = & \left[2.3278 - 0.001655 \mathcal{I}(R_{10}) + 0.0005 \mathcal{I}(R_{10}R_8^*) + 0.0524 \mathcal{I}(R_7) + 0.02266 \mathcal{I}(R_7R_8^*) \right. \\ & + 0.00496 \mathcal{I}(R_7R_9^*) + 0.00504 \mathcal{I}(R_8) + 0.0261 \mathcal{I}(R_8R_9^*) - 0.00651 \mathcal{I}(R_9) \\ & - 0.5426 \mathcal{R}(R_{10}) - 0.02578 \mathcal{R}(R_7) + 0.0153 \mathcal{R}(R_7R_{10}^*) + 0.0674 \mathcal{R}(R_7R_8^*) \\ & - 0.86996 \mathcal{R}(R_7R_9^*) - 0.0128 \mathcal{R}(R_8) + 0.00185 \mathcal{R}(R_8R_{10}^*) - 0.09926 \mathcal{R}(R_8R_9^*) \\ & + 2.841 \mathcal{R}(R_9) - 0.10705 \mathcal{R}(R_9R_{10}^*) + 11.0367 |R_{10}|^2 + 0.2813 |R_7|^2 \\ & \left. + 0.003765 |R_8|^2 + 1.528 |R_9|^2 \right] \times 10^{-7}, \end{aligned} \quad (13)$$

where (see Eqs. (18), (69), (70) for the Wilson coefficient definitions)

$$R_{7,8} = \frac{C_{7,8}^{(00)\text{eff}}(\mu_0)}{C_{7,8}^{(00)\text{eff,SM}}(\mu_0)} \quad \text{and} \quad R_{9,10} = \frac{C_{9,10}^{(11)}(\mu_0)}{C_{9,10}^{(11)\text{SM}}(\mu_0)}. \quad (14)$$

3 The effective theory

3.1 Operator basis

Resummation of large QCD logarithms is most conveniently performed in the framework of a low-energy effective theory [24]. There are ten operators that need to be considered at the leading order in the electroweak interactions. They can be chosen as follows:

$$\begin{aligned}
P_1 &= (\bar{s}_L \gamma_\mu T^a c_L)(\bar{c}_L \gamma^\mu T^a b_L), \\
P_2 &= (\bar{s}_L \gamma_\mu c_L)(\bar{c}_L \gamma^\mu b_L), \\
P_3 &= (\bar{s}_L \gamma_\mu b_L) \sum_q (\bar{q} \gamma^\mu q), \\
P_4 &= (\bar{s}_L \gamma_\mu T^a b_L) \sum_q (\bar{q} \gamma^\mu T^a q), \\
P_5 &= (\bar{s}_L \gamma_{\mu_1} \gamma_{\mu_2} \gamma_{\mu_3} b_L) \sum_q (\bar{q} \gamma^{\mu_1} \gamma^{\mu_2} \gamma^{\mu_3} q), \\
P_6 &= (\bar{s}_L \gamma_{\mu_1} \gamma_{\mu_2} \gamma_{\mu_3} T^a b_L) \sum_q (\bar{q} \gamma^{\mu_1} \gamma^{\mu_2} \gamma^{\mu_3} T^a q), \\
P_7 &= \frac{e}{16\pi^2} m_b (\bar{s}_L \sigma^{\mu\nu} b_R) F_{\mu\nu}, \\
P_8 &= \frac{g}{16\pi^2} m_b (\bar{s}_L \sigma^{\mu\nu} T^a b_R) G_{\mu\nu}^a, \\
P_9 &= (\bar{s}_L \gamma_\mu b_L) \sum_l (\bar{l} \gamma^\mu l), \\
P_{10} &= (\bar{s}_L \gamma_\mu b_L) \sum_l (\bar{l} \gamma^\mu \gamma_5 l).
\end{aligned} \tag{15}$$

In P_3, \dots, P_6 , the quark flavors are $q = u, d, s, c, b$. In P_9 and P_{10} , all the three lepton flavors are present. Contrary to other analyses [25, 26], we have not included any gauge couplings in the normalization of P_9 and P_{10} . Including them would give only a minor simplification in the present investigation.

Once QED corrections are considered, five more operators need to be taken into account. They can be chosen as

$$\begin{aligned}
P_{3Q} &= (\bar{s}_L \gamma_\mu b_L) \sum_q Q_q (\bar{q} \gamma^\mu q), \\
P_{4Q} &= (\bar{s}_L \gamma_\mu T^a b_L) \sum_q Q_q (\bar{q} \gamma^\mu T^a q), \\
P_{5Q} &= (\bar{s}_L \gamma_{\mu_1} \gamma_{\mu_2} \gamma_{\mu_3} b_L) \sum_q Q_q (\bar{q} \gamma^{\mu_1} \gamma^{\mu_2} \gamma^{\mu_3} q), \\
P_{6Q} &= (\bar{s}_L \gamma_{\mu_1} \gamma_{\mu_2} \gamma_{\mu_3} T^a b_L) \sum_q Q_q (\bar{q} \gamma^{\mu_1} \gamma^{\mu_2} \gamma^{\mu_3} T^a q), \\
P_b &= \frac{1}{12} \left[(\bar{s}_L \gamma_{\mu_1} \gamma_{\mu_2} \gamma_{\mu_3} b_L) (\bar{b} \gamma^{\mu_1} \gamma^{\mu_2} \gamma^{\mu_3} b) - 4(\bar{s}_L \gamma_\mu b_L) (\bar{b} \gamma^\mu b) \right].
\end{aligned} \tag{16}$$

where Q_q are the electric charges of the corresponding quarks ($\frac{2}{3}$ or $-\frac{1}{3}$).

The Lagrangian of the effective theory reads

$$\mathcal{L}_{eff} = \mathcal{L}_{QCD \times QED}(u, d, s, c, b, e, \mu, \tau) + \frac{4G_F}{\sqrt{2}} V_{ts}^* V_{tb} \left[\sum_{i=1}^{10} C_i(\mu) P_i + \sum_{i=3}^6 C_{iQ}(\mu) P_{iQ} + C_b(\mu) P_b \right]. \tag{17}$$

3.2 Matching conditions

The Wilson coefficients at the matching scale $\mu_0 \sim M_W, m_t$ are expanded as follows

$$\begin{aligned} C_k(\mu_0) &= C_k^{(00)}(\mu_0) + \tilde{\alpha}_s(\mu_0) C_k^{(10)}(\mu_0) + \tilde{\alpha}_s(\mu_0)^2 C_k^{(20)}(\mu_0) \\ &\quad + \tilde{\alpha}_s(\mu_0) \kappa(\mu_0) C_k^{(11)}(\mu_0) + \tilde{\alpha}_s(\mu_0)^2 \kappa(\mu_0) C_k^{(21)}(\mu_0) + \mathcal{O}(\tilde{\alpha}_s^3, \kappa^2 \tilde{\alpha}_s^2), \end{aligned} \quad (18)$$

where $\tilde{\alpha}_s = \alpha_s/4\pi$. Note, that at the low scale $\mu_b \sim m_b, m_{\ell\ell}$, also terms of order κ, κ^2 and $\kappa^2 \alpha_s$ arise and are included wherever necessary.

The values of the Wilson coefficients are found from the requirement that all the effective theory Green functions[†] match to the full SM ones at the leading order in M_L^2/M_H^2 . At the order we consider, the following non-vanishing contributions to Eq. (18) must be taken into account for the four-fermion operators ($s_W^2 \equiv \sin^2 \theta_W$):

$$C_2^{(00)}(\mu_0) = 1, \quad (19)$$

$$C_1^{(10)}(\mu_0) = 15 + 6 \ln \frac{\mu_0^2}{M_W^2}, \quad (20)$$

$$C_4^{(10)}(\mu_0) = E(x_t) - \frac{2}{3} + \frac{2}{3} \ln \frac{\mu_0^2}{M_W^2}, \quad (21)$$

$$C_2^{(11)}(\mu_0) = -\frac{7}{3} - \frac{4}{3} \ln \frac{\mu_0^2}{M_Z^2}, \quad (22)$$

$$C_3^{(11)}(\mu_0) = \frac{2}{9s_W^2} [X(x_t) - 2Y(x_t)], \quad (23)$$

$$C_5^{(11)}(\mu_0) = -\frac{1}{18s_W^2} [X(x_t) - 2Y(x_t)], \quad (24)$$

$$C_9^{(11)}(\mu_0) = \frac{1}{s_W^2} Y(x_t) + W(x_t) + \frac{4}{9} - \frac{4}{9} \ln \frac{\mu_0^2}{m_t^2}, \quad (25)$$

$$C_{10}^{(11)}(\mu_0) = -\frac{1}{s_W^2} Y(x_t), \quad (26)$$

$$C_{3Q}^{(11)}(\mu_0) = \frac{2}{3s_W^2} [X(x_t) + Y(x_t)] - W(x_t) - \frac{4}{9} + \frac{4}{9} \ln \frac{\mu_0^2}{m_t^2}, \quad (27)$$

$$C_{5Q}^{(11)}(\mu_0) = -\frac{1}{6s_W^2} [X(x_t) + Y(x_t)], \quad (28)$$

$$C_b^{(11)}(\mu_0) = -\frac{1}{2s_W^2} S(x_t), \quad (29)$$

$$C_i^{(20)}(\mu_0) = C_i^{t(2)}(\mu_0) - C_i^{c(2)}(\mu_0) \quad \text{for } i = 1, \dots, 6, \quad (30)$$

$$C_i^{(21)}(\mu_0) = C_i^{t(2)}(\mu_0) - C_i^{c(2)}(\mu_0) \quad \text{for } i = 9, 10, \quad (31)$$

[†]For the on-shell 1PR functions, the operators from Section 3.1 are sufficient. However, it is often more convenient find the Wilson coefficients by matching the off-shell 1PI functions. Then, additional operators are necessary — see Eq. (73) of Ref. [3].

$$C_9^{(22)}(\mu_0) = -\frac{x_t^2}{32s_W^4} (4s_W^2 - 1) \left[3 + \tau_b^{(2)}(x_{ht}) - \Delta_t(x_{ht}) \right], \quad (32)$$

$$C_{10}^{(22)}(\mu_0) = -\frac{x_t^2}{32s_W^4} \left[3 + \tau_b^{(2)}(x_{ht}) - \Delta_t(x_{ht}) \right]. \quad (33)$$

All the one-loop coefficients $C_i^{(1m)}(\mu_0)$ above have been evaluated in the $\overline{\text{MS}}$ scheme.[‡] The functions $E(x)$, $X(x)$, $Y(x)$, $W(x)$, $S(x)$ are collected in Appendix A. The one-loop coefficient $C_2^{(11)}$ is from Ref. [27]. The other one-loop ones have been known since many years (see, e.g., Ref. [28]). For $C_i^{(20)}$ and $C_i^{(21)}$, the relevant top ($C_i^{t(2)}$) and charm ($C_i^{c(2)}$) contributions to the two-loop matching conditions can be found in Section 2 of Ref. [3]. The functions $\tau_b^{(2)}$ and Δ_t , where $x_t \equiv (m_t^{\overline{\text{MS}}}/M_W)^2$ and $x_{ht} \equiv (M_h/m_t^{\overline{\text{MS}}})^2$, can be found in Ref. [29]. We include also the contributions to $C_{i(Q)}^{(21)}(\mu_0)$ that were calculated in Refs. [3, 30]. Transforming the results of Ref. [30] to our operator basis is non-trivial.[§]

3.3 Renormalization Group Equations

In the effective theory, the RGE for the gauge couplings read

$$\begin{aligned} \mu \frac{d\tilde{\alpha}_s}{d\mu} &= -2\tilde{\alpha}_s^2 \sum_{n,m=0} \beta_{nm}^s \tilde{\alpha}_s^n \tilde{\alpha}_e^m, \\ \mu \frac{d\tilde{\alpha}_e}{d\mu} &= +2\tilde{\alpha}_e^2 \sum_{n,m=0} \beta_{nm}^e \tilde{\alpha}_e^n \tilde{\alpha}_s^m, \end{aligned} \quad (34)$$

where $\tilde{\alpha}_e = \alpha_{\text{em}}/4\pi$. The solution for $\tilde{\alpha}_s(\mu)$ with the initial condition at $\mu = \mu_0$ is found perturbatively in $\tilde{\alpha}_s(\mu_0)$ and $\tilde{\alpha}_e(\mu_0)$ but exactly in $v_s = 1 + 2\beta_{00}^s \tilde{\alpha}_s(\mu_0) \ln \frac{\mu}{\mu_0}$ and $v_e = 1 - 2\beta_{00}^e \tilde{\alpha}_e(\mu_0) \ln \frac{\mu}{\mu_0}$. Including all the 3-loop contributions, and, in addition, the 4-loop pure-QCD term, one obtains

$$\begin{aligned} \tilde{\alpha}_s(\mu) &= \frac{\tilde{\alpha}_s(\mu_0)}{v_s} - \frac{\tilde{\alpha}_s(\mu_0)^2}{v_s^2} \left(\frac{\beta_{10}^s}{\beta_{00}^s} \ln v_s - \frac{\beta_{01}^s}{\beta_{00}^e} \ln v_e \right) + \frac{\tilde{\alpha}_s(\mu_0)^3}{v_s^3} \left[\frac{\beta_{20}^s}{\beta_{00}^s} (1 - v_s) \right. \\ &+ \left(\frac{\beta_{10}^s}{\beta_{00}^s} \right)^2 \left(\ln^2 v_s - \ln v_s + v_s - 1 \right) + \left(\frac{\beta_{01}^s}{\beta_{00}^e} \right)^2 \ln^2 v_e + \frac{\beta_{01}^s \beta_{10}^s}{\beta_{00}^s \beta_{00}^e} (-2 \ln v_s \ln v_e + \rho v_e \ln v_e) \Big] \\ &+ \frac{\tilde{\alpha}_s(\mu_0)^4}{v_s^4} \left[\frac{\beta_{30}^s}{\beta_{00}^s} \frac{1 - v_s^2}{2} + \frac{\beta_{20}^s \beta_{10}^s}{(\beta_{00}^s)^2} ((2v_s - 3) \ln v_s + v_s^2 - v_s) \right. \\ &+ \left. \left(\frac{\beta_{10}^s}{\beta_{00}^s} \right)^3 \left(-\ln^3 v_s + \frac{5}{2} \ln^2 v_s + 2(1 - v_s) \ln v_s - \frac{1}{2} (v_s - 1)^2 \right) \right] \end{aligned}$$

[‡]Beyond tree-level, the Wilson coefficients usually depend on the choice of evanescent operators. Our choice is the same as in Refs. [7–9].

[§]We thank Ulrich Haisch for providing us with the relevant transformation matrices.

$$\begin{aligned}
& + \frac{\tilde{\alpha}_s(\mu_0)^2 \tilde{\alpha}_e(\mu_0)}{v_s^2 v_e} \left[\frac{\beta_{02}^s}{\beta_{00}^e} (v_e - 1) + \frac{\beta_{11}^s}{\beta_{00}^s} \rho v_e \ln \frac{v_e}{v_s} + \frac{\beta_{01}^s \beta_{10}^e}{(\beta_{00}^e)^2} (\ln v_e - v_e + 1) \right. \\
& \left. + \frac{\beta_{01}^s \beta_{10}^e}{(\beta_{00}^s)^2} \rho \ln v_s + \frac{\beta_{01}^s \beta_{01}^e}{\beta_{00}^s \beta_{00}^e} \left(\rho v_e \ln \frac{v_s}{v_e} - \ln v_s \right) \right] + \tilde{\alpha}_s^2 \times \mathcal{O}(\tilde{\alpha}_s^3, \tilde{\alpha}_e^2, \tilde{\alpha}_s \tilde{\alpha}_e), \tag{35}
\end{aligned}$$

where $\rho = \beta_{00}^s \tilde{\alpha}_s(\mu_0) / (\beta_{00}^s \tilde{\alpha}_s(\mu_0) + \beta_{00}^e \tilde{\alpha}_e(\mu_0))$. The corresponding solution for $\tilde{\alpha}_e(\mu)$ can be found by obvious replacements: $v_s \leftrightarrow v_e$, $\tilde{\alpha}_s \leftrightarrow \tilde{\alpha}_e$ and $\beta_{ij}^s \leftrightarrow -\beta_{ij}^e$ (also inside the ratio ρ).

The $\overline{\text{MS}}$ values of the pure-QCD coefficients β_{ij}^s can be found in Refs. [31, 32]. After substituting $C_A = N = 3$, $C_F = \frac{4}{3}$, $t_F = \frac{1}{2}$ and $n_f = 5$, one finds $\beta_{00}^s = \frac{23}{3}$, $\beta_{10}^s = \frac{116}{3}$, $\beta_{20}^s = \frac{9769}{54}$ and $\beta_{30}^s = \frac{352864}{81} \zeta(3) - \frac{598391}{1458}$. The remaining beta-function coefficients that enter into Eq. (35) read[¶]

$$\begin{aligned}
\beta_{01}^s &= -4t_F \overline{Q^2} = -\frac{22}{9}, & \beta_{00}^e &= \frac{4}{3} \left(\overline{Q^2} N + 3Q_l^2 \right) = \frac{80}{9}, \\
\beta_{11}^s &= (4C_F - 8C_A) t_F \overline{Q^2} = -\frac{308}{27}, & \beta_{10}^e &= 4 \left(\overline{Q^4} N + 3Q_l^4 \right) = \frac{464}{27}, \\
\beta_{02}^s &= \frac{11}{3} t_F \overline{Q^2} \beta_{00}^e + 2t_F \overline{Q^4} = \frac{4945}{243}, & \beta_{01}^e &= 4C_F N \overline{Q^2} = \frac{176}{9},
\end{aligned} \tag{36}$$

where $Q_l = -1$, $Q_u = \frac{2}{3}$, $Q_d = -\frac{1}{3}$ and $\overline{Q^n} = 2Q_u^n + 3Q_d^n$.

The RGE for the Wilson coefficients reads

$$\mu \frac{d}{d\mu} \vec{C}(\mu) = \hat{\gamma}^T(\mu) \vec{C}(\mu), \tag{37}$$

where the Anomalous Dimension Matrix (ADM) has the following expansion:

$$\hat{\gamma}(\mu) = \sum_{\substack{n, m=0 \\ n+m \geq 1}} \hat{\gamma}^{(nm)} \tilde{\alpha}_s(\mu)^n \tilde{\alpha}_e(\mu)^m. \tag{38}$$

In Eq. (35), we have made no use of the fact that $\tilde{\alpha}_e \ll \tilde{\alpha}_s$. Now we shall take this relation into account, and solve the RGE (37) perturbatively in

$$\lambda \equiv \frac{\beta_{00}^e \tilde{\alpha}_e(\mu_0)}{\beta_{00}^s \tilde{\alpha}_s(\mu_0)} \quad \text{and} \quad \omega \equiv 2\beta_{00}^s \tilde{\alpha}_s(\mu_0), \tag{39}$$

neglecting terms of order $\mathcal{O}(\omega^3, \lambda^3, \omega^2 \lambda^2)$. Let us introduce the following short-hand notation:

$$\begin{aligned}
b_1 &= \frac{\beta_{10}^s}{2(\beta_{00}^s)^2}, & b_2 &= \frac{\beta_{20}^s}{4(\beta_{00}^s)^3} - b_1^2, & b_3 &= \frac{\beta_{01}^s}{2\beta_{00}^s \beta_{00}^e}, \\
b_4 &= \frac{\beta_{11}^s}{4(\beta_{00}^s)^2 \beta_{00}^e} - 2b_1 b_3, & b_5 &= \frac{\beta_{01}^e}{2\beta_{00}^s \beta_{00}^e} - b_1, & \hat{W}^{(nm)} &= \frac{(\hat{\gamma}^{(nm)})^T}{(2\beta_{00}^s)^n (2\beta_{00}^e)^m}.
\end{aligned} \tag{40}$$

[¶]All of them except β_{11}^s can be found by modifying the color and charge factors in the pure QCD results. As far as β_{11}^s is concerned, we have found it by performing an explicit three-loop calculation. To our knowledge, no result for this coefficient has been published before.

The known evolution of the gauge couplings (35) allows us to rewrite the RGE (37) in terms of the variable $\eta = \tilde{\alpha}_s(\mu_0)/\tilde{\alpha}_s(\mu)$

$$\frac{d}{d\eta} \vec{C} = \frac{1}{\eta} \left[\hat{W}^{(10)} + \sum_{k=-2}^2 \hat{B}^{(k)} \eta^k + \lambda^2 \omega b_5 \hat{W}^{(01)} \eta \ln \eta + \mathcal{O}(\omega^3, \lambda^3, \omega^2 \lambda^2) \right] \vec{C}. \quad (41)$$

where the matrices $\hat{B}^{(k)}$ are η -independent

$$\hat{B}^{(-2)} = \omega^2 \left(\hat{W}^{(30)} - b_1 \hat{W}^{(20)} - b_2 \hat{W}^{(10)} \right), \quad (42)$$

$$\hat{B}^{(-1)} = \omega \left(\hat{W}^{(20)} - b_1 \hat{W}^{(10)} \right) + \omega^2 \lambda \left(\hat{W}^{(21)} - b_1 \hat{W}^{(11)} - b_2 \hat{W}^{(01)} - b_3 \hat{W}^{(20)} - b_4 \hat{W}^{(10)} \right), \quad (43)$$

$$\hat{B}^{(0)} = \omega \lambda (1 - \lambda) \left(\hat{W}^{(11)} - b_1 \hat{W}^{(01)} - b_3 \hat{W}^{(10)} \right), \quad (44)$$

$$\hat{B}^{(1)} = \lambda (1 - \lambda) \hat{W}^{(01)} + \omega \lambda^2 \left(\hat{W}^{(02)} + \hat{W}^{(11)} - (b_1 + b_3) \hat{W}^{(01)} - b_3 \hat{W}^{(10)} \right), \quad (45)$$

$$\hat{B}^{(2)} = \lambda^2 \hat{W}^{(01)}. \quad (46)$$

The solution to Eq. (41) reads

$$\begin{aligned} \vec{C}(\mu) = \hat{V} \left[\hat{D}(\eta) + \sum_{k=-2}^2 \hat{F}^{(k)}(\eta) + \sum_{k,l=-2}^2 \hat{G}^{(kl)}(\eta) \right. \\ \left. + \sum_{k,l,m=-2}^2 \hat{H}^{(klm)}(\eta) + \hat{R}(\eta) + \mathcal{O}(\omega^3, \lambda^3, \omega^2 \lambda^2) \right] \hat{V}^{-1} \vec{C}(\mu_0), \end{aligned} \quad (47)$$

where \hat{V} is the matrix that diagonalizes $\hat{W}^{(10)}$

$$\left[\hat{V}^{-1} \hat{W}^{(10)} \hat{V} \right]_{ij} = a_{\underline{i}} \delta_{ij}. \quad (48)$$

The eigenvalues a_i and entries of the matrix \hat{V} are given numerically in appendix B. The matrices $\hat{D}(\eta)$, $\hat{F}^{(k)}(\eta)$, $\hat{G}^{(kl)}(\eta)$, $\hat{H}^{(klm)}(\eta)$ and $\hat{R}(\eta)$ depend on the a_i and on products $\hat{E}^{(k)} \equiv \hat{V}^{-1} \hat{B}^{(k)} \hat{V}$. They read

$$\begin{aligned} \hat{D}_{ij}(\eta) &= \eta^{a_i} \delta_{ij}, & \hat{F}_{ij}^{(k)}(\eta) &= \hat{E}_{ij}^{(k)} f_{\underline{i}\underline{j}}^{(k)}(\eta), & \hat{G}_{ij}^{(kl)}(\eta) &= \sum_p \hat{E}_{ip}^{(k)} \hat{E}_{pj}^{(l)} g_{\underline{i}\underline{p}\underline{j}}^{(kl)}(\eta), \\ \hat{H}_{ij}^{(klm)}(\eta) &= \sum_{p,q} \hat{E}_{ip}^{(k)} \hat{E}_{pq}^{(l)} \hat{E}_{qj}^{(m)} h_{\underline{i}\underline{p}\underline{q}\underline{j}}^{(klm)}(\eta), & \hat{R}_{ij}(\eta) &= \lambda^2 \omega b_5 \left(\hat{V}^{-1} \hat{W}^{(01)} \hat{V} \right)_{ij} r_{\underline{i}\underline{j}}^{(1)}(\eta). \end{aligned} \quad (49)$$

The functions $f_{ij}^{(k)}(\eta)$, $g_{ipj}^{(kl)}(\eta)$, $h_{ipqj}^{(klm)}(\eta)$ and $r_{ij}^{(k)}(\eta)$ are given by

$$f_{ij}^{(k)}(\eta) = \begin{cases} \eta^{a_i} \ln \eta, & \text{when } a_j + k - a_i = 0, \\ \frac{1}{a_j + k - a_i} \left(\eta^{a_j + k} - \eta^{a_i} \right), & \text{otherwise,} \end{cases} \quad (50)$$

$$r_{ij}^{(k)}(\eta) = \begin{cases} \frac{1}{2} \eta^{a_i} \ln^2 \eta, & \text{when } a_j + k - a_i = 0, \\ \frac{1}{a_j + k - a_i} \left(\eta^{a_j + k} \ln \eta - f_{ij}^{(k)}(\eta) \right), & \text{otherwise,} \end{cases} \quad (51)$$

$$g_{ipj}^{(kl)}(\eta) = \begin{cases} r_{ip}^{(k)}(\eta) & \text{when } a_j + l - a_p = 0, \\ \frac{1}{a_j + l - a_p} (f_{ij}^{(k+l)}(\eta) - f_{ip}^{(k)}(\eta)), & \text{otherwise,} \end{cases} \quad (52)$$

$$h_{ipqj}^{(klm)}(\eta) = \begin{cases} \frac{1}{6} \eta^{a_i} \ln^3 \eta, & \text{when } a_p + k - a_i = a_q + l - a_p = a_j + m - a_q = 0, \\ \frac{1}{a_p + k - a_i} \left(\frac{1}{2} \eta^{a_p+k} \ln^2 \eta - r_{ip}^{(k)}(\eta) \right), & \text{when } a_p + k - a_i \neq 0 \text{ and } a_q + l - a_p = a_j + m - a_q = 0, \\ \frac{1}{a_q + l - a_p} \left(r_{iq}^{(k+l)}(\eta) - g_{ipq}^{(kl)}(\eta) \right), & \text{when } a_q + l - a_p \neq 0 \text{ and } a_j + m - a_q = 0, \\ \frac{1}{a_j + m - a_q} \left(g_{ipj}^{(k,l+m)}(\eta) - g_{ipq}^{(kl)}(\eta) \right), & \text{when } a_j + m - a_q \neq 0. \end{cases} \quad (53)$$

3.4 Anomalous dimension matrices

In the present Section, we give the ADM's for the four-fermion operators. When the operators are ordered as in the list $\{P_1, \dots, P_6, P_9, P_{10}, P_{3Q}, \dots, P_{6Q}, P_b\}$, then the matrices that enter Eq. (38) have the following generic structure:

$$\hat{\gamma}^{(nm)} = \begin{bmatrix} (\hat{\gamma}_{CC}^{(nm)})_{2 \times 2} & (\hat{\gamma}_{CP}^{(nm)})_{2 \times 4} & (\hat{\gamma}_{CL}^{(nm)})_{2 \times 2} & (\hat{\gamma}_{CQ}^{(nm)})_{2 \times 4} & 0_{2 \times 1} \\ 0_{4 \times 2} & (\hat{\gamma}_{PP}^{(nm)})_{4 \times 4} & (\hat{\gamma}_{PL}^{(nm)})_{4 \times 2} & (\hat{\gamma}_{PQ}^{(nm)})_{4 \times 4} & 0_{4 \times 1} \\ 0_{2 \times 2} & (\hat{\gamma}_{LP}^{(nm)})_{2 \times 4} & (\hat{\gamma}_{LL}^{(nm)})_{2 \times 2} & (\hat{\gamma}_{LQ}^{(nm)})_{2 \times 4} & 0_{2 \times 1} \\ 0_{4 \times 2} & (\hat{\gamma}_{QP}^{(nm)})_{4 \times 4} & (\hat{\gamma}_{QL}^{(nm)})_{4 \times 2} & (\hat{\gamma}_{QQ}^{(nm)})_{4 \times 4} & 0_{4 \times 1} \\ 0_{1 \times 2} & (\hat{\gamma}_{BP}^{(nm)})_{1 \times 4} & (\hat{\gamma}_{BL}^{(nm)})_{1 \times 2} & (\hat{\gamma}_{BQ}^{(nm)})_{1 \times 4} & (\hat{\gamma}_{BB}^{(nm)})_{1 \times 1} \end{bmatrix}. \quad (54)$$

However, the pure-QCD ADM's have a much simpler structure

$$\hat{\gamma}^{(n0)} = \begin{bmatrix} (\hat{\gamma}_{CC}^{(n0)})_{2 \times 2} & (\hat{\gamma}_{CP}^{(n0)})_{2 \times 4} & 0_{2 \times 2} & 0_{2 \times 4} & 0_{2 \times 1} \\ 0_{4 \times 2} & (\hat{\gamma}_{PP}^{(n0)})_{4 \times 4} & 0_{4 \times 2} & 0_{4 \times 4} & 0_{4 \times 1} \\ 0_{2 \times 2} & 0_{2 \times 4} & 0_{2 \times 2} & 0_{2 \times 4} & 0_{2 \times 1} \\ 0_{4 \times 2} & (\hat{\gamma}_{QP}^{(n0)})_{4 \times 4} & 0_{1 \times 2} & (\hat{\gamma}_{QQ}^{(n0)})_{4 \times 4} & 0_{4 \times 1} \\ 0_{1 \times 2} & (\hat{\gamma}_{BP}^{(n0)})_{1 \times 4} & 0_{1 \times 2} & 0_{1 \times 4} & (\hat{\gamma}_{BB}^{(n0)})_{1 \times 1} \end{bmatrix}. \quad (55)$$

Moreover, four additional blocks vanish in $\hat{\gamma}^{(01)}$

$$\hat{\gamma}_{CP}^{(01)} = 0, \quad \hat{\gamma}_{PP}^{(01)} = 0, \quad \hat{\gamma}_{LP}^{(01)} = 0, \quad \hat{\gamma}_{BP}^{(01)} = 0. \quad (56)$$

We need to know all the non-vanishing blocks of $\hat{\gamma}^{(10)}$ and $\hat{\gamma}^{(20)}$:

$$\hat{\gamma}_{CC}^{(10)} = \begin{bmatrix} -4 & \frac{8}{3} \\ 12 & 0 \end{bmatrix}, \quad \hat{\gamma}_{CP}^{(10)} = \begin{bmatrix} 0 & -\frac{2}{9} & 0 & 0 \\ 0 & \frac{4}{3} & 0 & 0 \end{bmatrix}, \quad \hat{\gamma}_{PP}^{(10)} = \begin{bmatrix} 0 & -\frac{52}{3} & 0 & 2 \\ -\frac{40}{9} & -\frac{100}{9} & \frac{4}{9} & \frac{5}{6} \\ 0 & -\frac{256}{3} & 0 & 20 \\ -\frac{256}{9} & \frac{56}{9} & \frac{40}{9} & -\frac{2}{3} \end{bmatrix},$$

$$\hat{\gamma}_{QP}^{(10)} = \begin{bmatrix} 0 & -\frac{8}{9} & 0 & 0 \\ 0 & \frac{16}{27} & 0 & 0 \\ 0 & -\frac{128}{9} & 0 & 0 \\ 0 & \frac{184}{27} & 0 & 0 \end{bmatrix}, \quad \hat{\gamma}_{QQ}^{(10)} = \begin{bmatrix} 0 & -20 & 0 & 2 \\ -\frac{40}{9} & -\frac{52}{3} & \frac{4}{9} & \frac{5}{6} \\ 0 & -128 & 0 & 20 \\ -\frac{256}{9} & -\frac{160}{3} & \frac{40}{9} & -\frac{2}{3} \end{bmatrix}, \quad \hat{\gamma}_{BB}^{(10)} = [4], \quad (57)$$

$$\hat{\gamma}_{BP}^{(10)} = \begin{bmatrix} 0 & \frac{4}{3} & 0 & 0 \end{bmatrix},$$

$$\hat{\gamma}_{CC}^{(20)} = \begin{bmatrix} -\frac{355}{9} & -\frac{502}{27} \\ -\frac{35}{3} & -\frac{28}{3} \end{bmatrix}, \quad \hat{\gamma}_{CP}^{(20)} = \begin{bmatrix} -\frac{1412}{243} & -\frac{1369}{243} & \frac{134}{243} & -\frac{35}{162} \\ -\frac{416}{81} & \frac{1280}{81} & \frac{56}{81} & \frac{35}{27} \end{bmatrix},$$

$$\hat{\gamma}_{PP}^{(20)} = \begin{bmatrix} -\frac{4468}{81} & -\frac{31469}{81} & \frac{400}{81} & \frac{3373}{108} \\ -\frac{8158}{243} & -\frac{59399}{243} & \frac{269}{486} & \frac{12899}{648} \\ -\frac{251680}{81} & -\frac{128648}{243} & \frac{23836}{81} & \frac{6106}{27} \\ \frac{58640}{243} & -\frac{26348}{243} & -\frac{14324}{243} & -\frac{2551}{162} \end{bmatrix}, \quad \hat{\gamma}_{QP}^{(20)} = \begin{bmatrix} \frac{832}{243} & -\frac{4000}{243} & -\frac{112}{243} & -\frac{70}{81} \\ \frac{3376}{729} & \frac{6344}{729} & -\frac{280}{729} & \frac{55}{486} \\ \frac{2272}{243} & -\frac{72088}{243} & -\frac{688}{243} & -\frac{1240}{81} \\ \frac{45424}{729} & \frac{84236}{729} & -\frac{3880}{729} & \frac{1220}{243} \end{bmatrix},$$

$$\hat{\gamma}_{QQ}^{(20)} = \begin{bmatrix} -\frac{404}{9} & -\frac{3077}{9} & \frac{32}{9} & \frac{1031}{36} \\ -\frac{2698}{81} & -\frac{8035}{27} & -\frac{49}{162} & \frac{4493}{216} \\ -\frac{19072}{9} & -\frac{14096}{27} & \frac{1708}{9} & \frac{1622}{9} \\ \frac{32288}{81} & -\frac{15976}{27} & -\frac{6692}{81} & -\frac{2437}{54} \end{bmatrix}, \quad \hat{\gamma}_{BP}^{(20)} = \begin{bmatrix} -\frac{1576}{81} & \frac{446}{27} & \frac{172}{81} & \frac{40}{27} \end{bmatrix}, \quad (58)$$

$$\hat{\gamma}_{BB}^{(20)} = \begin{bmatrix} \frac{325}{9} \end{bmatrix}.$$

Almost all the blocks of $\hat{\gamma}^{(01)}$ are necessary:

$$\hat{\gamma}_{BL}^{(01)} = \begin{bmatrix} \frac{16}{9} & 0 \end{bmatrix},$$

$$\hat{\gamma}_{CC}^{(01)} = \begin{bmatrix} -\frac{8}{3} & 0 \\ 0 & -\frac{8}{3} \end{bmatrix}, \quad \hat{\gamma}_{CL}^{(01)} = \begin{bmatrix} -\frac{32}{27} & 0 \\ -\frac{8}{9} & 0 \end{bmatrix}, \quad \hat{\gamma}_{CQ}^{(01)} = \begin{bmatrix} \frac{32}{27} & 0 & 0 & 0 \\ \frac{8}{9} & 0 & 0 & 0 \end{bmatrix}, \quad \hat{\gamma}_{LL}^{(01)} = \begin{bmatrix} 8 & -4 \\ -4 & 0 \end{bmatrix},$$

$$\hat{\gamma}_{PQ}^{(01)} = \begin{bmatrix} \frac{76}{9} & 0 & -\frac{2}{3} & 0 \\ -\frac{32}{27} & \frac{20}{3} & 0 & -\frac{2}{3} \\ \frac{496}{9} & 0 & -\frac{20}{3} & 0 \\ -\frac{512}{27} & \frac{128}{3} & 0 & -\frac{20}{3} \end{bmatrix}, \quad \hat{\gamma}_{PL}^{(01)} = \begin{bmatrix} -\frac{16}{9} & 0 \\ \frac{32}{27} & 0 \\ -\frac{112}{9} & 0 \\ \frac{512}{27} & 0 \end{bmatrix}, \quad \hat{\gamma}_{QL}^{(01)} = \begin{bmatrix} -\frac{272}{27} & 0 \\ -\frac{32}{81} & 0 \\ -\frac{2768}{27} & 0 \\ -\frac{512}{81} & 0 \end{bmatrix}. \quad (59)$$

From $\hat{\gamma}^{(02)}$ we need only the mixing of P_1, \dots, P_6 into P_9 and P_{10} :

$$\hat{\gamma}_{CL}^{(02)} = \begin{bmatrix} -\frac{11680}{2187} & -\frac{416}{81} \\ -\frac{2920}{729} & -\frac{104}{27} \end{bmatrix}, \quad \hat{\gamma}_{PL}^{(02)} = \begin{bmatrix} -\frac{39752}{729} & -\frac{136}{27} \\ \frac{1024}{2187} & -\frac{448}{81} \\ -\frac{381344}{729} & -\frac{15616}{27} \\ \frac{24832}{2187} & -\frac{7936}{81} \end{bmatrix}. \quad (60)$$

The necessary entries of $\hat{\gamma}^{(11)}$ read:

$$\hat{\gamma}_{CC}^{(11)} = \begin{bmatrix} \frac{169}{9} & \frac{100}{27} \\ \frac{50}{3} & -\frac{8}{3} \end{bmatrix}, \quad \hat{\gamma}_{CP}^{(11)} = \begin{bmatrix} 0 & \frac{254}{729} & 0 & 0 \\ 0 & \frac{1076}{243} & 0 & 0 \end{bmatrix}, \quad \hat{\gamma}_{CQ}^{(11)} = \begin{bmatrix} \frac{2272}{729} & \frac{122}{81} & 0 & \frac{49}{81} \\ -\frac{1952}{243} & -\frac{748}{27} & 0 & \frac{82}{27} \end{bmatrix},$$

$$\begin{aligned}
\hat{\gamma}_{PP}^{(11)} &= \begin{bmatrix} 0 & \frac{11116}{243} & 0 & -\frac{14}{3} \\ \frac{280}{27} & \frac{18763}{729} & -\frac{28}{27} & -\frac{35}{18} \\ 0 & \frac{111136}{243} & 0 & -\frac{140}{3} \\ \frac{2944}{27} & \frac{193312}{729} & -\frac{280}{27} & -\frac{175}{9} \end{bmatrix}, \quad \hat{\gamma}_{PQ}^{(11)} = \begin{bmatrix} -\frac{23488}{243} & \frac{6280}{27} & \frac{112}{9} & -\frac{538}{27} \\ \frac{31568}{729} & \frac{9481}{81} & -\frac{92}{27} & -\frac{1012}{81} \\ -\frac{233920}{243} & \frac{68848}{27} & \frac{1120}{9} & -\frac{5056}{27} \\ \frac{352352}{729} & \frac{116680}{81} & -\frac{752}{27} & -\frac{10147}{81} \end{bmatrix}, \\
\hat{\gamma}_{PL}^{(11)} &= \begin{bmatrix} -\frac{6752}{243} & 0 \\ -\frac{2192}{729} & 0 \\ -\frac{84032}{243} & 0 \\ -\frac{37856}{729} & 0 \end{bmatrix}, \quad \hat{\gamma}_{QL}^{(11)} = \begin{bmatrix} -\frac{24352}{729} & 0 \\ \frac{54608}{2187} & 0 \\ -\frac{227008}{729} & 0 \\ \frac{551648}{2187} & 0 \end{bmatrix}, \quad \hat{\gamma}_{CL}^{(11)} = \begin{bmatrix} -\frac{2272}{729} & 0 \\ \frac{1952}{243} & 0 \end{bmatrix}, \quad \hat{\gamma}_{LL}^{(11)} = \begin{bmatrix} 0 & 16 \\ 16 & 0 \end{bmatrix}, \\
\hat{\gamma}_{BL}^{(11)} &= \begin{bmatrix} -\frac{8}{9} & 0 \end{bmatrix}. \tag{61}
\end{aligned}$$

Finally, the relevant 3-loop anomalous dimensions yield [8]

$$\hat{\gamma}_{CC}^{(30)} = \begin{bmatrix} -\frac{12773}{18} + \frac{1472\zeta(3)}{3} & \frac{745}{9} - \frac{4288\zeta(3)}{9} \\ \frac{1177}{2} - 2144\zeta(3) & 306 - 224\zeta(3) \end{bmatrix}, \quad \hat{\gamma}_{CL}^{(21)} = \begin{bmatrix} -\frac{1359190}{19683} + \frac{6976\zeta(3)}{243} & 0 \\ -\frac{229696}{6561} - \frac{3584\zeta(3)}{81} & 0 \end{bmatrix}, \tag{62}$$

$$\hat{\gamma}_{CP}^{(30)} = \begin{bmatrix} \frac{63187}{13122} & -\frac{981796}{6561} & -\frac{202663}{52488} & -\frac{24973}{69984} \\ \frac{110477}{2187} & \frac{133529}{8748} & -\frac{42929}{8748} & \frac{354319}{11664} \end{bmatrix} + \zeta(3) \begin{bmatrix} -\frac{1360}{81} & -\frac{776}{81} & \frac{124}{81} & \frac{100}{27} \\ \frac{2720}{27} & -\frac{2768}{27} & -\frac{248}{27} & -\frac{110}{9} \end{bmatrix}, \tag{63}$$

$$\begin{aligned}
\hat{\gamma}_{PP}^{(30)} &= \begin{bmatrix} -\frac{3572528}{2187} & -\frac{58158773}{8748} & \frac{552601}{4374} & \frac{6989171}{11664} \\ -\frac{1651004}{6561} & -\frac{155405353}{52488} & \frac{1174159}{52488} & \frac{10278809}{34992} \\ -\frac{147978032}{2187} & -\frac{168491372}{2187} & \frac{11213042}{2187} & \frac{17850329}{2916} \\ \frac{136797922}{6561} & -\frac{72614473}{13122} & -\frac{9288181}{6561} & -\frac{16664027}{17496} \end{bmatrix} \\
&+ \zeta(3) \begin{bmatrix} -\frac{608}{27} & \frac{61424}{27} & -\frac{496}{27} & -\frac{2821}{9} \\ \frac{88720}{81} & \frac{54272}{81} & -\frac{9274}{27} & -\frac{3100}{27} \\ \frac{87040}{27} & \frac{324416}{27} & -\frac{13984}{27} & -\frac{31420}{9} \\ \frac{721408}{81} & -\frac{166432}{81} & -\frac{95032}{81} & -\frac{7552}{27} \end{bmatrix}, \tag{64}
\end{aligned}$$

$$+\zeta(3) \begin{bmatrix} -\frac{1290092}{6561} + \frac{3200\zeta(3)}{81} & 0 \\ -\frac{819971}{19683} - \frac{19936\zeta(3)}{243} & 0 \\ -\frac{16821944}{6561} + \frac{30464\zeta(3)}{81} & 0 \\ -\frac{17787368}{19683} - \frac{286720\zeta(3)}{243} & 0 \end{bmatrix}. \tag{65}$$

The three-loop ADM's have no influence on the logarithmically-enhanced QED corrections at the considered order but are necessary for the NNLO QCD corrections. As far as the one- and two-loop ADM's are concerned, we have calculated all of them, and our results agree with Ref. [9].

3.5 Wilson coefficients at the low scale

From the solution to the RGE in Section 3.3, we obtain the Wilson coefficients at the scale $\mu_b \sim m_b$ as truncated series in $\tilde{\alpha}_s(\mu_0)$ and $\kappa(\mu_0)$. We then use Eq. (35) to express the couplings at the high scale in terms of $\tilde{\alpha}_s(\mu_b)$ and $\kappa(\mu_b)$. For $\tilde{\alpha}_s$, the simple relation

$$\tilde{\alpha}_s(\mu_0) = \eta \tilde{\alpha}_s(\mu_b) \tag{66}$$

holds to all orders. In order to obtain the running of κ , we invert Eq. (35), treating v_s and η as quantities of order $\mathcal{O}(1)$, which gives

$$\kappa(\mu_0) = \frac{\kappa(\mu_b)}{\eta} + \frac{\beta_{00}^e}{\beta_{00}^s} \frac{1-\eta}{\eta^2} \kappa^2(\mu_b) + \frac{\ln \eta}{\eta} \left[\frac{\beta_{00}^e \beta_{10}^s}{(\beta_{00}^s)^2} - \frac{\beta_{01}^e}{\beta_{00}^s} \right] \tilde{\alpha}_s(\mu_b) \kappa^2(\mu_b) + \mathcal{O}(\kappa^2 \tilde{\alpha}_s^2, \kappa^3). \quad (67)$$

The final expression for the Wilson coefficients at the low scale is:

$$C_k(\mu_b) = \sum_{n,m=0}^2 \tilde{\alpha}_s(\mu_b)^n \kappa(\mu_b)^m C_k^{(nm)}(\mu_b) + \mathcal{O}(\tilde{\alpha}_s^3, \kappa^3), \quad (68)$$

where $\vec{C}^{(n,m)}$ are functions of only $\eta = \tilde{\alpha}_s(\mu_0)/\tilde{\alpha}_s(\mu_b)$, s_W^2 and ratios of the heavy masses. At order $\mathcal{O}(\tilde{\alpha}_s^2 \kappa^2)$, we keep only those contributions to C_9 and C_{10} that are proportional to $m_t^4/(M_W^4 s_W^4)$.

The matching conditions, anomalous dimensions and RG-equations presented in Sections 3.2–3.4 do not include the two dipole operators $P_{7,8}$. For those two operators, it is more convenient to consider the so-called effective coefficients

$$\begin{aligned} C_7^{\text{eff}}(\mu_b) &\equiv C_7(\mu_b) + \sum_{i=3}^6 y_i \left[C_i(\mu_b) - \frac{1}{3} C_{iQ}(\mu_b) \right] \\ &= C_7^{(00)\text{eff}}(\mu_b) + \tilde{\alpha}_s(\mu_b) C_7^{(10)\text{eff}}(\mu_b) + \kappa(\mu_b) C_7^{(01)\text{eff}}(\mu_b) \\ &\quad + \tilde{\alpha}_s(\mu_b) \kappa(\mu_b) C_7^{(11)\text{eff}}(\mu_b) + \mathcal{O}(\tilde{\alpha}_s^2, \kappa^2), \end{aligned} \quad (69)$$

$$C_8^{\text{eff}}(\mu_b) \equiv C_8(\mu_b) + \sum_{i=3}^6 z_i \left[C_i(\mu_b) - \frac{1}{3} C_{iQ}(\mu_b) \right] = C_8^{(00)\text{eff}}(\mu_b) + \mathcal{O}(\tilde{\alpha}_s, \kappa) \quad (70)$$

where, in dimensional regularization with fully anticommuting γ_5 , $y = (0, 0, -\frac{1}{3}, -\frac{4}{9}, -\frac{20}{3}, -\frac{80}{9})$ and $z = (0, 0, 1, -\frac{1}{6}, 20, -\frac{10}{3})$. The effective coefficients $C_7^{(00)\text{eff}}(\mu_b)$, $C_7^{(10)\text{eff}}(\mu_b)$ and $C_8^{(00)\text{eff}}(\mu_b)$ can be found in Eqs. (10)–(22) of Ref. [33], while $C_7^{(01)\text{eff}}(\mu_b)$ can be found in Eq. (12) of Ref. [34].

Following Ref. [9], we take into account the *complete* $\mathcal{O}(\tilde{\alpha}_s \kappa)$ term in $C_7^{\text{eff}}(\mu_b)$ rather than only its $m_t^2/(M_W^2 s_W^2)$ -enhanced part (as Section 2 would imply). An explicit expression for $C_7^{(11)\text{eff}}(\mu_b)$ can be found in Eq. (30) of Ref. [27]. In Tables 3 – 5, we present the relevant $C_k^{(nm)}(\mu_b)$. We fix the input parameters to their central values (specified in sec. 2) and choose $\mu_b = [2.5, 5, 10]$ GeV and $\mu_0 = 120$ GeV.

4 Matrix elements I

Once $\vec{C}^{(n,m)}(\mu_b)$ is found, one needs to calculate the on-shell $b \rightarrow sl^+l^-$ matrix elements $\langle P_i \rangle$ of the corresponding operators. In the present section, we consider those parts of the matrix elements that originate from diagrams with no photons inside loops and/or bremsstrahlung photons. These parts are unrelated to the $\ln(m_b^2/m_\ell^2)$ -enhanced correction to the decay width.

	(00)	(01)	(10)
$C_1^{(nm)}$	[-0.763 , -0.544 , -0.379]	[-0.180, -0.0835, -0.0378]	[13.764 , 14.943 , 16.066]
$C_2^{(nm)}$	[1.054 , 1.029 , 1.015]	[0.248, 0.158, 0.101]	[-1.746 , -1.376 , -1.050]
$C_3^{(nm)}$	[-1.10 , -0.571 , -0.283] 10^{-2}	[-1.22, -0.400, -0.125] 10^{-3}	[5.28 , 7.98 , 8.38] 10^{-2}
$C_4^{(nm)}$	[-0.113 , -0.0741 , -0.0486]	[-1.62, -0.697, -0.297] 10^{-2}	[-0.690 , -0.343 , -0.143]
$C_5^{(nm)}$	[1.04 , 0.547 , 0.274] 10^{-3}	[1.17, 0.387, 0.122] 10^{-4}	[-1.60 , -1.55 , -1.36] 10^{-2}
$C_6^{(nm)}$	[2.32 , 1.17 , 0.563] 10^{-3}	[2.51, 0.801, 0.245] 10^{-4}	[-0.656 , -1.92 , -2.17] 10^{-2}
$C_{3Q}^{(nm)}$	0	[-5.03, -3.72, -2.66] 10^{-2}	0
$C_{4Q}^{(nm)}$	0	[-2.13, -1.04, -0.49] 10^{-2}	0
$C_{5Q}^{(nm)}$	0	[-6.08, -1.71, -0.30] 10^{-6}	0
$C_{6Q}^{(nm)}$	0	[2.12, 1.03, 0.485] 10^{-3}	0
$C_b^{(nm)}$	0	0	0

Table 3: Numerical values of the relevant $C_k^{(nm)}(\mu_b)$ ($k \neq 7, 8, 9, 10$) for $\mu_b = [2.5, 5, 10]$ GeV.

	$C_7^{(nm)}(\mu_b)$	$C_8^{(nm)}(\mu_b)$
(00)	[-0.362 , -0.320 , -0.285]	[-0.168 , -0.151 , -0.138]
(01)	[3.20 , 3.33 , 2.82] 10^{-2}	—
(10)	[1.625 , 1.171 , 0.690]	—
(11)	[4.132 , 4.314 , 4.397]	—

Table 4: Numerical values of the relevant $C_{7,8}^{(nm)}(\mu_b)$ for $\mu_b = [2.5, 5, 10]$ GeV.

One-loop penguin contractions of the 4-fermion operators give the following contributions to the matrix elements:

$$\langle P_i \rangle^{\text{peng}} = M_i^9 \langle P_9 \rangle_{\text{tree}} + M_i^7 \frac{\langle P_7 \rangle_{\text{tree}}}{\tilde{\alpha}_s(\mu_b) \kappa(\mu_b)} + M_i^{10} \langle P_{10} \rangle_{\text{tree}}. \quad (71)$$

The above formula holds also for the tree-level matrix element of P_7 , the one-loop matrix element of P_8 , and for those parts of the two-loop $\mathcal{O}(\alpha_s \alpha_{\text{em}})$ matrix elements of the 4-quark operators where the gluon couples to the closed quark loop. The coefficients M_i^A are summarized in Table 6 in terms of the functions $F_i^A(\hat{s})$ and

$$f_i(\hat{s}) = \gamma_{i9}^{(01)} \ln \frac{m_b}{\mu_b} + \rho_i^c \left(g(y_c) + \frac{8}{9} \ln \frac{m_b}{m_c} \right) + \rho_i^b g(y_b) + \rho_i^0 (\ln \hat{s} - i\pi) + \rho_i^\# , \quad (72)$$

$$f_9^{\text{pen}}(\hat{s}) = 8 \ln \frac{m_b}{\mu_b} - 3 \left(g(y_\tau) + \frac{8}{9} \ln \frac{m_b}{m_\tau} \right) + \frac{8}{3} (\ln \hat{s} - i\pi) - \frac{40}{9} . \quad (73)$$

Here, $y_a = 4m_{a,\text{pole}}^2/m_{\ell^+\ell^-}^2$, the function $g(y)$ is given in Appendix A, and the numbers ρ are collected in Table 7. The functions $F_i^A(\hat{s})$ can be found in Eqs. (54)–(56), (71) and (72) of

	$C_9^{(nm)}(\mu_b)$	$C_{10}^{(nm)}(\mu_b)$
(00)	0	0
(01)	$[5.025, 3.722, 2.664] 10^{-2}$	0
(10)	0	0
(11)	$[2.003, 1.934, 1.863]$	$[-4.222, -4.222, -4.222]$
(20)	0	0
(02)	$[0.376, 0.208, 0.104] 10^{-2}$	$[1.081, 0.489, 0.218] 10^{-2}$
(12)	$[-6.614, -4.317, -2.810]$	$[-5.854, -3.798, -2.458]$
(21)	$[5.645, 3.538, 1.193]$	$[5.105, 6.380, 7.631]$
(22)	$[36.814, 27.320, 20.275]$	$[-32.014, -36.090, -39.764]$

Table 5: Numerical values of the relevant $C_{9,10}^{(nm)}(\mu_b)$ for $\mu_b = [2.5, 5, 10]$ GeV.

	M_i^9	M_i^7	M_i^{10}
i=1,2	$\tilde{\alpha}_s \kappa f_i(\hat{s}) - \tilde{\alpha}_s^2 \kappa F_i^9(\hat{s})$	$-\tilde{\alpha}_s^2 \kappa F_i^7(\hat{s})$	0
i=3-6,3Q-6Q,b	$\tilde{\alpha}_s \kappa f_i(\hat{s})$	0	0
i=7	0	$\tilde{\alpha}_s \kappa$	0
i=8	$-\tilde{\alpha}_s^2 \kappa F_8^9(\hat{s})$	$-\tilde{\alpha}_s^2 \kappa F_8^7(\hat{s})$	0
i=9	$1 + \tilde{\alpha}_s \kappa f_9^{\text{pen}}(\hat{s})$	0	0
i=10	0	0	1

Table 6: Coefficients M_i^A that appear in Eq. (71). Here, $\tilde{\alpha}_s$ and κ are taken at the scale μ_b .

Ref. [4] where they are given in terms of an expansion in \hat{s} up to $\mathcal{O}(\hat{s}^3)$. In the range of \hat{s} that we consider here, the accuracy of these expansions is excellent, as can be seen in Fig. 8 of Ref. [6] where the same functions are numerically evaluated for arbitrary \hat{s} .

For what concerns the remaining contributions to the NLO and NNLO QCD matrix elements of $P_{7,9,10}$, the virtual and real corrections can be effectively taken into account via the following redefinitions of the squared tree-level matrix elements in the expression for the decay width:

$$|\langle P_9 \rangle_{\text{tree}}|^2 \implies |\langle P_9 \rangle_{\text{tree}}|^2 \left[1 + 8 \tilde{\alpha}_s \omega_{99}^{(1)}(\hat{s}) + 16 \tilde{\alpha}_s^2 \omega_{99}^{(2)}(\hat{s}) \right], \quad (74)$$

$$|\langle P_{10} \rangle_{\text{tree}}|^2 \implies |\langle P_{10} \rangle_{\text{tree}}|^2 \left[1 + 8 \tilde{\alpha}_s \omega_{1010}^{(1)}(\hat{s}) \right], \quad (75)$$

$$|\langle P_7 \rangle_{\text{tree}}|^2 \implies |\langle P_7 \rangle_{\text{tree}}|^2 \left[1 + 8 \tilde{\alpha}_s \omega_{77}^{(1)}(\hat{s}) \right], \quad (76)$$

$$\text{Re}(\langle P_7 \rangle_{\text{tree}} \langle P_9 \rangle_{\text{tree}}^*) \implies \text{Re}(\langle P_7 \rangle_{\text{tree}} \langle P_9 \rangle_{\text{tree}}^*) \left[1 + 8 \tilde{\alpha}_s \omega_{79}^{(1)}(\hat{s}) \right], \quad (77)$$

where the functions $\omega_{ij}^{(n)}(\hat{s})$ calculated in Refs. [4, 9] are listed in Appendix A.

The remaining contributions to the NNLO matrix elements of the 4-quark operators originate from diagrams where the gluon does not couple to the quark loop. Thus, they are given by the same functions of \hat{s} as in Eq. (74).

	P_1	P_2	P_3	P_4	P_5	P_6	P_3^Q	P_4^Q	P_5^Q	P_6^Q	P^b
ρ^c	$\frac{4}{3}$	1	6	0	60	0	4	0	40	0	0
ρ^b	0	0	$-\frac{7}{2}$	$-\frac{2}{3}$	-38	$-\frac{32}{3}$	$\frac{7}{6}$	$\frac{2}{9}$	$\frac{38}{3}$	$\frac{32}{9}$	-2
ρ^0	0	0	$\frac{2}{9}$	$\frac{8}{27}$	$\frac{32}{9}$	$\frac{128}{27}$	$-\frac{74}{27}$	$-\frac{8}{81}$	$-\frac{752}{27}$	$-\frac{128}{81}$	0
$\rho^\#$	$-\frac{16}{27}$	$-\frac{4}{9}$	$\frac{2}{27}$	$\frac{8}{81}$	$-\frac{136}{27}$	$\frac{320}{81}$	$\frac{358}{81}$	$-\frac{8}{243}$	$\frac{1144}{81}$	$-\frac{320}{243}$	$\frac{26}{27}$

Table 7: Numbers that occur in the four-quark operator matrix elements in Eq. (72).

5 Matrix elements II

In this Section, we calculate those electromagnetic corrections to the matrix elements of the 4-fermion operators that are responsible for the $\ln(m_b^2/m_\ell^2)$ -enhanced correction to the decay width. In section 5.1, we cover in great detail the calculation of QED corrections to $\langle P_9 \rangle$. In Section 5.2, we give the logarithmically enhanced QED corrections to the matrix elements of P_i with $i \neq 9$.

5.1 Corrections to $\langle P_9 \rangle$

Electromagnetic corrections to the matrix element of P_9 are infrared divergent and must be considered together with the corresponding bremsstrahlung. The dilepton invariant mass differential decay width is not an infrared safe object with respect to emission of collinear photons. Hence, electromagnetic corrections contain an explicit collinear logarithm $\ln(m_b^2/m_\ell^2)$. The coefficient of this logarithm vanishes when integrated over the whole phase space but not if we restrict it to the low- \hat{s} region.

In this calculation, we adopt the NDR scheme with $D = 4 - 2\epsilon$. The NDR scheme is suitable for our calculation since no Levi-Civita tensor survives in divergent terms proportional to $1/\epsilon$ or $1/\epsilon^2$. Thus, all the Levi-Civita tensors can be evaluated in $D = 4$ and are therefore well-defined.

In the first step, all the external particles are taken to be on-shell, and, in addition, all the final state particles are treated as massless ($m_s = m_\ell = 0$). This implies that all the collinear divergences are dimensionally regularized, and that the collinear logarithm appears as a residual $1/\epsilon$. Later, we will be able to re-express such a residue in terms of $\ln(m_b^2/m_\ell^2)$ using the photonic splitting function of the lepton.

In the next two subsections, we present the calculation of virtual and bremsstrahlung corrections. In the last one, we show how to change the collinear regulator from dimensional to the physical mass regularization.

The calculation involves the following kinematical invariants: $\hat{s}_{ij} = 2 \frac{p_i \cdot p_j}{m_b^2}$ where $i, j \in \{l^+, l^-, s, b, \gamma\} \equiv \{1, 2, s, b, q\}$.

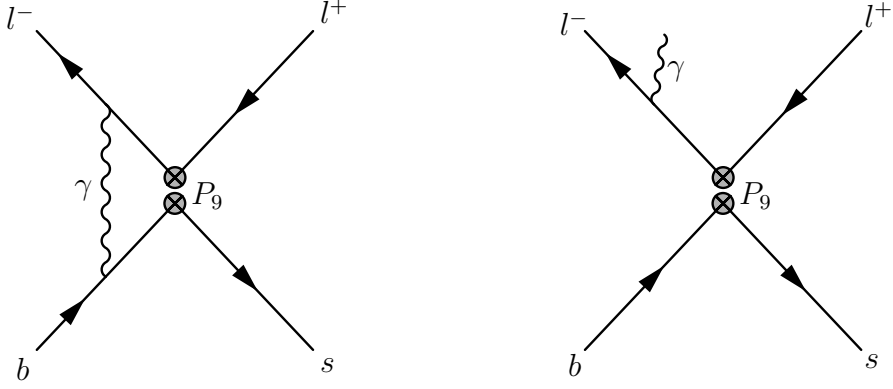


Figure 1: Examples of diagrams contributing to the virtual (left) and real (right) electromagnetic corrections to the matrix element of P_9 .

5.1.1 Virtual corrections

In order to obtain the virtual corrections, one has to consider one-loop diagrams of the current-current type. There are in total six such diagrams, one of which is shown on the left in Figure 1. The sum of the six amplitudes contains infrared and ultraviolet divergences. The latter cancel after the addition of counterterms. The next step is then to compute its interference with $\langle P_9 \rangle_{\text{tree}}$ which yields an expression $K_V(\hat{s}_{12}, \hat{s}_{1s}, \hat{s}_{2s})$. Finally, one has to integrate K_V over the phase space. The phase space measure for a three particle massless final state in D dimensions is given explicitly in [35]. Since K_V does not depend on angular variables we can immediately integrate them out

$$\begin{aligned} \widetilde{dPS}_3 &\equiv \tilde{\mu}^{4\epsilon} \int_{\Omega} dPS_3 = \tilde{\mu}^{4\epsilon} M_3(\hat{s}_{12}, \hat{s}_{1s}, \hat{s}_{2s}) d\hat{s}_{12} d\hat{s}_{1s} d\hat{s}_{2s} \\ &= \tilde{\mu}^{4\epsilon} \frac{2^{-8+6\epsilon} \pi^{-\frac{5}{2}+2\epsilon} (m_b^2)^{1-2\epsilon}}{\Gamma(\frac{3}{2}-\epsilon) \Gamma(1-\epsilon)} (\hat{s}_{12} \hat{s}_{1s} \hat{s}_{2s})^{-\epsilon} \delta(1 - \hat{s}_{12} - \hat{s}_{1s} - \hat{s}_{2s}) d\hat{s}_{12} d\hat{s}_{1s} d\hat{s}_{2s}. \end{aligned} \quad (78)$$

By means of this expression we obtain the final contribution from virtual corrections via

$$T_V \equiv \int \frac{d\widetilde{PS}_3}{d\hat{s}_{12}} K_V(\hat{s}_{12}, \hat{s}_{1s}, \hat{s}_{2s}). \quad (79)$$

5.1.2 Real corrections

In order to cancel the infrared singularities present in T_V one has to add the corresponding bremsstrahlung contribution. There are four diagrams, one of which is shown on the right in Figure 1. Contrary to the case of gluon bremsstrahlung, the photon couples to all external legs, which makes the calculation more involved. The sum of the four amplitudes has to be squared, yielding an expression $K_R(\hat{s}_{12}, \hat{s}_{1s}, \hat{s}_{2s}, \hat{s}_{1q}, \hat{s}_{2q}, \hat{s}_{sq}, \hat{s}_{tri})$, where

$$\hat{s}_{tri} \equiv 1 - \hat{s}_{12} - \hat{s}_{1s} - \hat{s}_{2s} = \hat{s}_{1q} + \hat{s}_{2q} + \hat{s}_{sq} \quad (80)$$

is the triple invariant. The corresponding phase space measure for the four particle final state can also be found in [35]. After integration over angular variables, it reads

$$\begin{aligned} d\widetilde{PS}_4 \equiv \tilde{\mu}^{6\epsilon} \int_{\Omega} dPS_4 &= \tilde{\mu}^{6\epsilon} \cdot \frac{2^{-12+10\epsilon} \pi^{-5+3\epsilon} (m_b^2)^{2-3\epsilon}}{\Gamma(\frac{3}{2}-\epsilon) \Gamma(1-\epsilon) \Gamma(\frac{1}{2}-\epsilon)} d\hat{s}_{12} d\hat{s}_{1s} d\hat{s}_{1q} d\hat{s}_{2s} d\hat{s}_{2q} d\hat{s}_{sq} \\ &\times (-\Delta_4)^{-\frac{1}{2}-\epsilon} \cdot \Theta(-\Delta_4) \cdot \delta(1 - \hat{s}_{12} - \hat{s}_{1s} - \hat{s}_{1q} - \hat{s}_{2s} - \hat{s}_{2q} - \hat{s}_{sq}). \end{aligned} \quad (81)$$

In the above equation, the Gram determinant is given by

$$\Delta_4 = (\hat{s}_{12}\hat{s}_{sq})^2 + (\hat{s}_{1s}\hat{s}_{2q})^2 + (\hat{s}_{1q}\hat{s}_{2s})^2 - 2(\hat{s}_{12}\hat{s}_{1s}\hat{s}_{2q}\hat{s}_{sq} + \hat{s}_{1s}\hat{s}_{1q}\hat{s}_{2s}\hat{s}_{2q} + \hat{s}_{12}\hat{s}_{1q}\hat{s}_{2s}\hat{s}_{sq}). \quad (82)$$

The phase space measure is completely symmetric in $\{1, 2, s, q\}$, but since we stay differential in \hat{s}_{12} we can only make use of the symmetries $1 \leftrightarrow 2$ and $s \leftrightarrow q$.^{||} The use of these symmetries is, however, essential since the number of distinct terms in K_R gets reduced significantly. In addition, all terms of the form $A/(\hat{s}_{1q}\hat{s}_{sq})$ and $A/(\hat{s}_{2q}\hat{s}_{sq})$ as well as $B/(\hat{s}_{1q}\hat{s}_{tri})$ and $B/(\hat{s}_{2q}\hat{s}_{tri})$ drop out by means of the $1 \leftrightarrow 2$ symmetry.

Another crucial point is to choose for each term in K_R the order of integration in a suitable way in order to ensure that all terms up to and including order ϵ^0 can be found analytically. Appendix C is devoted to this rather technical issue. The QED bremsstrahlung contribution finally reads

$$T_R \equiv \int \frac{d\widetilde{PS}_4}{d\hat{s}_{12}} K_R(\hat{s}_{12}, \hat{s}_{1s}, \hat{s}_{2s}, \hat{s}_{1q}, \hat{s}_{2q}, \hat{s}_{sq}, \hat{s}_{tri}). \quad (83)$$

In the sum of T_V and T_R the $1/\epsilon^2$ terms cancel as well as the Q_d^2 part of the $1/\epsilon$ terms, whereas the collinear divergences proportional to Q_l^2/ϵ remain.

5.1.3 From NDR to mass regularization

As we have stated earlier, the differential decay width is not an infrared safe object with respect to emission of collinear photons. This means that, as long as the lepton is treated as massless, the sum of virtual and real corrections is not free of collinear divergences. If we had kept the lepton mass different from zero during the whole calculation, the sum of virtual and real corrections would have been finite. However, the computation of the diagrams and the massive phase space integrals in T_V and T_R would have been much more tedious.

The translation of the $1/\epsilon$ pole into a $\ln(m_b^2/m_\ell^2)$ corresponds to changing the regularization scheme and is complicated by the presence of soft infrared singularities. The correct procedure is to start with constructing an observable that is infrared safe and, consequently, regularization scheme independent. Only at this point we can switch to the m_ℓ regulator and obtain our final result. As an intermediate step, we construct a differential branching ratio where \hat{s} is identified as follows:

$$\hat{s} = \begin{cases} (p_{\ell_1} + p_{\ell_2} + p_\gamma)^2/m_b^2 & \text{if } \vec{p}_\gamma \parallel (\vec{p}_{\ell_1} \text{ or } \vec{p}_{\ell_2}) \\ (p_{\ell_1} + p_{\ell_2})^2/m_b^2 & \text{otherwise.} \end{cases} \quad (84)$$

^{||}In the terms containing \hat{s}_{tri} in the denominator, only the $1 \leftrightarrow 2$ symmetry can be used.

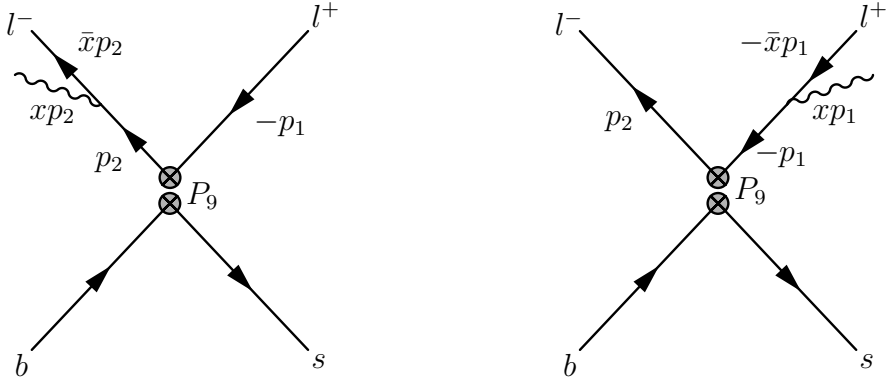


Figure 2: Splitting function kinematics. The photon is emitted by a quasi-real lepton.

In order to switch to this intermediate observable we must subtract the *collinear* decay width differential in the dilepton invariant mass and add the same quantity but remaining differential in the triple invariant.

The calculation of the differential branching ratio in the collinear limit is done with the help of the NDR-scheme splitting function for the massless lepton. The splitting function in this scheme can be derived from Refs. [36, 37] and reads

$$f_\gamma^{(\epsilon)}(x, E) = 4\tilde{\alpha}_e \left[\frac{1 + (1-x)^2}{x} \left(-\frac{1}{2\epsilon} + \ln \frac{E}{\mu} + \ln(2-2x) \right) - \frac{(2-x)^2}{2x} \ln \frac{2-x}{x} \right], \quad (85)$$

where E is the energy of the incoming lepton and xE is the energy of the emitted photon. See Fig. 2 for a pictorial view of the kinematics.

The fully differential decay width in the collinear limit is given by (here and in the following we omit the factor $8G_F^2|V_{tb}V_{ts}|^2$ stemming from the effective Lagrangian):

$$\begin{aligned} d\Gamma_{\text{coll}}^{(\epsilon)}(\hat{s}_{12}, \hat{s}_{1s}, \hat{s}_{2s}, x) &= (2m_b)^{-1} \left[f_\gamma^{(\epsilon)}(x, E_1) + f_\gamma^{(\epsilon)}(x, E_2) \right] |\langle P_9 \rangle_{\text{tree}}|^2 dPS_3 dx \\ &= m_b^{-1} f_\gamma^{(\epsilon)}(x, E_1) |\langle P_9 \rangle_{\text{tree}}|^2 dPS_3 dx, \end{aligned} \quad (86)$$

where $x, \hat{s}_{12}, \hat{s}_{1s}, \hat{s}_{2s} \in [0, 1]$, $E_1 = m_b(1 - \hat{s}_{2s})/2$ and we used the $\ell_1 \leftrightarrow \ell_2$ symmetry. The collinear decay width differential in the triple invariant ($\hat{s} = (p_{\ell_1} + p_{\ell_2} + p_\gamma)^2/m_b^2$) reads

$$\frac{d\Gamma_{\text{coll},3}^{(\epsilon)}}{d\hat{s}} = m_b^{-1} \int_0^1 dx \int_0^1 d\hat{s}_{1s} \int_0^1 d\hat{s}_{2s} M_3(\hat{s}, \hat{s}_{1s}, \hat{s}_{2s}) f_\gamma^{(\epsilon)}(x, E_1) |\langle P_9 \rangle_{\text{tree}}|_{\hat{s}_{12} \rightarrow \hat{s}}^2. \quad (87)$$

The collinear decay width differential in the dilepton invariant mass ($\hat{s} = (p_1 + \bar{x}p_2)^2/m_b^2$) reads

$$\frac{d\Gamma_{\text{coll},2}^{(\epsilon)}}{d\hat{s}} = m_b^{-1} \int_0^{1-\hat{s}} \frac{dx}{\bar{x}} \int_0^1 d\hat{s}_{1s} \int_0^1 d\hat{s}_{2s} M_3(\hat{s}/\bar{x}, \hat{s}_{1s}, \hat{s}_{2s}) f_\gamma^{(\epsilon)}(x, E_1) |\langle P_9 \rangle_{\text{tree}}|_{\hat{s}_{12} \rightarrow \hat{s}/\bar{x}}^2, \quad (88)$$

where $\bar{x} = 1 - x$, and the non-linear change of variables $\hat{s}_{12} \rightarrow \hat{s}/\bar{x}$ also implied a distortion of the x -integration domain. The addition of $\frac{d\Gamma_{\text{coll},3}^{(\epsilon)}}{d\hat{s}} - \frac{d\Gamma_{\text{coll},2}^{(\epsilon)}}{d\hat{s}}$ to the results of previous subsections removes the remaining ϵ -pole from the differential decay width.

We are now free to convert back this observable to the usual one (in which \hat{s} is always the dilepton invariant mass) using mass regularization. To this extent, we need the splitting function in this scheme [36]:

$$f_\gamma^{(m)}(x, E) = 4\tilde{\alpha}_e \left[\frac{1 + (1 - x)^2}{x} \left(\ln \frac{E}{m_\ell} + \ln(2 - 2x) \right) - 1 + x - \frac{x^2}{2} \ln x - \frac{(2 - x)^2}{2} \ln(2 - x) \right]. \quad (89)$$

The original differential decay width is then obtained by adding $\frac{d\Gamma_{\text{coll},2}^{(m)}}{d\hat{s}} - \frac{d\Gamma_{\text{coll},3}^{(m)}}{d\hat{s}}$ where $d\Gamma^{(m)}$ is obtained from $d\Gamma^{(\epsilon)}$ via $f_\gamma^{(\epsilon)} \rightarrow f_\gamma^{(m)}$. Therefore, the total correction term is given by the following double difference:

$$\frac{T_S}{2m_b} = \left(\frac{d\Gamma_{\text{coll},2}^{(m)}}{d\hat{s}} - \frac{d\Gamma_{\text{coll},2}^{(\epsilon)}}{d\hat{s}} \right) - \left(\frac{d\Gamma_{\text{coll},3}^{(m)}}{d\hat{s}} - \frac{d\Gamma_{\text{coll},3}^{(\epsilon)}}{d\hat{s}} \right). \quad (90)$$

Note that only the E -independent difference $f_\gamma^{(\epsilon)}(x, E) - f_\gamma^{(m)}(x, E)$ enters in the total correction term. Hence, we can perform separately the (x, \hat{s}_{12}) and $(\hat{s}_{1s}, \hat{s}_{2s})$ integrations. The tree level squared matrix element of P_9 integrated over the phase space reads

$$\sigma(\hat{s}_{12}) \equiv \frac{2^{-7+6\epsilon} \pi^{-\frac{5}{2}+2\epsilon} (m_b^2)^{3-2\epsilon} \tilde{\mu}^{4\epsilon}}{\Gamma(\frac{3}{2} - \epsilon)} d\hat{s}_{12} \hat{s}_{12}^{-\epsilon} (1 - \hat{s}_{12})^{2-2\epsilon} \frac{\Gamma(2 - \epsilon)}{\Gamma(2 - 2\epsilon)} \frac{2\hat{s}_{12}(1 - \epsilon) + 1}{3 - 2\epsilon} \quad (91)$$

and the total correction term is finally expressed as

$$T_S = 2 \left[\int_0^1 dx \left[f_\gamma^{(\epsilon)}(x) - f_\gamma^{(m)}(x) \right] \sigma(\hat{s}) - \int_0^{1-\hat{s}} dx \frac{f_\gamma^{(\epsilon)}(x) - f_\gamma^{(m)}(x)}{(1 - x)} \sigma\left(\frac{\hat{s}}{1 - x}\right) \right] \quad (92)$$

Both integrals in Eq. (92) are infrared divergent for $x \rightarrow 0$, but their sum is not.

The sum $T_V + T_R + T_S$ is now free of divergences and contains an explicit collinear logarithm $\ln(m_b^2/m_\ell^2)$. The coefficient of this logarithm vanishes when integrated over \hat{s}_{12} . This means that if we had considered the total branching ratio instead of the differential one, the sum of $T_V + T_R$ would have been already finite and the inclusion of T_S would have become unnecessary. However, the coefficient of the collinear logarithm is large and positive for low \hat{s}_{12} and large and negative for high \hat{s}_{12} . Furthermore, this term renders by far the major contribution to the electromagnetic corrections. In the sum $T_V + T_R + T_S$ the coefficient of Q_d^2 is up to a color factor proportional to the QCD-function $\omega_{99}^{(1)}(\hat{s})$ from Eq. (127), providing another check for our result. Inserting $Q_d = -1/3$ and $Q_l = -1$ finally yields

$$T_V + T_R + T_S = \frac{\tilde{\alpha}_e m_b^6 (1 - \hat{s}_{12})^2 (1 + 2\hat{s}_{12})}{24\pi^3} \omega_{99}^{(\text{em})}(\hat{s}_{12}), \quad (93)$$

with

$$\begin{aligned} \omega_{99}^{(\text{em})}(\hat{s}) = & \ln\left(\frac{m_b^2}{m_\ell^2}\right) \left[-\frac{1 + 4\hat{s} - 8\hat{s}^2}{6(1 - \hat{s})(1 + 2\hat{s})} + \ln(1 - \hat{s}) - \frac{(1 - 6\hat{s}^2 + 4\hat{s}^3) \ln \hat{s}}{2(1 - \hat{s})^2(1 + 2\hat{s})} \right] \\ & - \frac{1}{9} Li_2(\hat{s}) + \frac{4}{27}\pi^2 - \frac{121 - 27\hat{s} - 30\hat{s}^2}{72(1 - \hat{s})(1 + 2\hat{s})} - \frac{(41 + 76\hat{s}) \ln(1 - \hat{s})}{36(1 + 2\hat{s})} \\ & + \left(\frac{-3 - 10\hat{s} - 17\hat{s}^2 + 14\hat{s}^3}{18(1 - \hat{s})^2(1 + 2\hat{s})} + \frac{17 \ln(1 - \hat{s})}{18} \right) \ln \hat{s} - \frac{(1 - 6\hat{s}^2 + 4\hat{s}^3) \ln^2 \hat{s}}{2(1 - \hat{s})^2(1 + 2\hat{s})}. \end{aligned} \quad (94)$$

The contribution that we have calculated can be effectively taken into account via the following substitution:

$$|C_9(\mu_b)\langle P_9 \rangle_{\text{tree}}|^2 \implies |C_9(\mu_b)\langle P_9 \rangle_{\text{tree}}|^2 \left[1 + 8 \tilde{\alpha}_e \omega_{99}^{(\text{em})}(\hat{s}) \right]. \quad (95)$$

5.2 Other log-enhanced corrections

The QED corrections to the matrix elements of P_i with $i \neq 9$ contribute to the branching ratio at order $O(\tilde{\alpha}_s^3 \kappa^3)$. Consequently, following the outline in Section 2, we include those contributions that are enhanced by an explicit $\ln(m_b/m_\ell)$. The relevant terms in the amplitude are

$$\mathcal{A} \propto \left[(C_2 + C_F C_1) \tilde{\alpha}_s \kappa f_2(\hat{s}) + C_9 \right] \langle P_9 \rangle_{\text{tree}} + C_{10} \langle P_{10} \rangle_{\text{tree}} + C_7 \langle P_7 \rangle_{\text{tree}} \quad (96)$$

where the $f_2(\hat{s})$ is defined in Eq. (72). Here we have dropped the NNLO QCD corrections to the matrix elements as well as the terms proportional to the small penguin coefficients $C_{i(Q)}$. After squaring and under the assumption that C_1 and C_2 are real, we obtain

$$\begin{aligned} |\mathcal{A}|^2 \propto & \left[|C_9|^2 + \tilde{\alpha}_s^2 \kappa^2 (C_2 + C_F C_1)^2 |f_2(\hat{s})|^2 + 2 \tilde{\alpha}_s \kappa \text{Re}[f_2(\hat{s})(C_2 + C_F C_1)C_9^*] \right] |\langle P_9 \rangle_{\text{tree}}|^2 \\ & + 2 \text{Re} \left[C_7 C_9^* + \tilde{\alpha}_s \kappa C_7 (C_2 + C_F C_1) f_2^*(\hat{s}) \right] \langle P_7 \rangle_{\text{tree}} \langle P_9 \rangle_{\text{tree}}^* \\ & + |C_7|^2 |\langle P_7 \rangle_{\text{tree}}|^2 + |C_{10}|^2 |\langle P_{10} \rangle_{\text{tree}}|^2. \end{aligned} \quad (97)$$

The fully differential decay width in the collinear limit now yields

$$d\Gamma_{\text{coll}}^{(m)}(\hat{s}_{12}, \hat{s}_{1s}, \hat{s}_{2s}, x) = m_b^{-1} f_\gamma^{(m)}(x, E_1) |\mathcal{A}|^2 dPS_3 dx. \quad (98)$$

These corrections are induced by collinear photon emission and are given by $\frac{d\Gamma_{\text{coll},2}^{(m)}}{d\hat{s}} - \frac{d\Gamma_{\text{coll},3}^{(m)}}{d\hat{s}}$ where we retain only the $\ln(m_b/m_\ell)$ term in $f_\gamma^{(m)}(x, E)$. The result reads

$$\begin{aligned} \frac{d\Delta\Gamma}{d\hat{s}} = & \frac{G_F^2 m_b^5}{48\pi^3} |V_{tb} V_{ts}|^2 (1 - \hat{s})^2 \tilde{\alpha}_s \kappa \left\{ 8(1 + 2\hat{s}) \left[|C_9|^2 \omega_{99}^{(\text{em})}(\hat{s}) + |C_{10}|^2 \omega_{1010}^{(\text{em})}(\hat{s}) \right. \right. \\ & + \tilde{\alpha}_s \kappa \text{Re} \left[(C_2 + C_F C_1) C_9^* \omega_{29}^{(\text{em})}(\hat{s}) \right] + \tilde{\alpha}_s^2 \kappa^2 (C_2 + C_F C_1)^2 \omega_{22}^{(\text{em})}(\hat{s}) \left. \right] \\ & + 96 \left[\tilde{\alpha}_s \kappa \text{Re} [C_7 C_9^*] \omega_{79}^{(\text{em})}(\hat{s}) + \tilde{\alpha}_s^2 \kappa^2 \text{Re} [(C_2 + C_F C_1) C_7^* \omega_{27}^{(\text{em})}(\hat{s})] \right] \\ & \left. \left. + 8 \left(4 + \frac{8}{\hat{s}} \right) \tilde{\alpha}_s^2 \kappa^2 |C_7|^2 \omega_{77}^{(\text{em})}(\hat{s}) \right\}, \right. \end{aligned} \quad (99)$$

where $\omega_{99}^{(\text{em})}(\hat{s})$ was already found in the previous section. The other ω -functions read:

$$\omega_{1010}^{(\text{em})}(\hat{s}) = \ln \left(\frac{m_b^2}{m_\ell^2} \right) \left[-\frac{1 + 4\hat{s} - 8\hat{s}^2}{6(1 - \hat{s})(1 + 2\hat{s})} + \ln(1 - \hat{s}) - \frac{(1 - 6\hat{s}^2 + 4\hat{s}^3) \ln \hat{s}}{2(1 - \hat{s})^2(1 + 2\hat{s})} \right], \quad (100)$$

$$\omega_{77}^{(\text{em})}(\hat{s}) = \ln\left(\frac{m_b^2}{m_\ell^2}\right) \left[\frac{\hat{s}}{2(1-\hat{s})(2+\hat{s})} + \ln(1-\hat{s}) - \frac{\hat{s}(-3+2\hat{s}^2)}{2(1-\hat{s})^2(2+\hat{s})} \ln(\hat{s}) \right], \quad (101)$$

$$\omega_{79}^{(\text{em})}(\hat{s}) = \ln\left(\frac{m_b^2}{m_\ell^2}\right) \left[-\frac{1}{2(1-\hat{s})} + \ln(1-\hat{s}) + \frac{(-1+2\hat{s}-2\hat{s}^2)}{2(1-\hat{s})^2} \ln(\hat{s}) \right], \quad (102)$$

$$\omega_{29}^{(\text{em})}(\hat{s}) = \ln\left(\frac{m_b^2}{m_\ell^2}\right) \left[\frac{\Sigma_1(\hat{s}) + i\Sigma_1^I(\hat{s})}{8(1-\hat{s})^2(1+2\hat{s})} \right] + \frac{16}{9} \omega_{1010}^{(\text{em})}(\hat{s}) \ln\left(\frac{\mu_b}{5\text{GeV}}\right), \quad (103)$$

$$\begin{aligned} \omega_{22}^{(\text{em})}(\hat{s}) = & \ln\left(\frac{m_b^2}{m_\ell^2}\right) \left[\frac{\Sigma_2(\hat{s})}{8(1-\hat{s})^2(1+2\hat{s})} + \frac{\Sigma_1(\hat{s})}{9(1-\hat{s})^2(1+2\hat{s})} \ln\left(\frac{\mu_b}{5\text{GeV}}\right) \right] \\ & + \frac{64}{81} \omega_{1010}^{(\text{em})}(\hat{s}) \ln^2\left(\frac{\mu_b}{5\text{GeV}}\right), \end{aligned} \quad (104)$$

$$\omega_{27}^{(\text{em})}(\hat{s}) = \ln\left(\frac{m_b^2}{m_\ell^2}\right) \left[\frac{\Sigma_3(\hat{s}) + i\Sigma_3^I(\hat{s})}{96(1-\hat{s})^2} \right] + \frac{8}{9} \omega_{79}^{(\text{em})}(\hat{s}) \ln\left(\frac{\mu_b}{5\text{GeV}}\right). \quad (105)$$

The functions Σ_i have been evaluated numerically in the low- \hat{s} -region (for fixed values of m_b and m_c):

$$\Sigma_1(\hat{s}) = 23.787 - 120.948\hat{s} + 365.373\hat{s}^2 - 584.206\hat{s}^3, \quad (106)$$

$$\Sigma_1^I(\hat{s}) = 1.653 + 6.009\hat{s} - 17.080\hat{s}^2 + 115.880\hat{s}^3, \quad (107)$$

$$\Sigma_2(\hat{s}) = 11.488 - 36.987\hat{s} + 255.330\hat{s}^2 - 812.388\hat{s}^3 + 1011.791\hat{s}^4, \quad (108)$$

$$\Sigma_3(\hat{s}) = 109.311 - 846.039\hat{s} + 2890.115\hat{s}^2 - 4179.072\hat{s}^3, \quad (109)$$

$$\Sigma_3^I(\hat{s}) = 4.606 + 17.650\hat{s} - 53.244\hat{s}^2 + 348.069\hat{s}^3. \quad (110)$$

6 Collinear logarithms and angular cuts

The explicit logarithm of the lepton mass signals the presence of a collinear singularity whose appearance in the differential branching ratio is strictly related to the definition of the dilepton invariant mass. As explained in Sec. 5.1.3, this logarithm disappears if all photons emitted by the final state on-shell leptons are included in the definition of s : $(p_{\ell_1} + p_{\ell_2})^2 \rightarrow (p_{\ell_1} + p_{\ell_2} + p_\gamma)^2$.

Let us consider a cone (of angular opening θ) around an on-shell lepton with momentum p_ℓ . For all photons emitted in this cone we have: $m_\ell^2 \leq (p_\ell + p_\gamma)^2 \leq \Lambda^2 \simeq 2E_\ell^2(1 - \cos\theta)$, where E_ℓ is the energy of the lepton (usually of order m_b). Consequently the effect of including such photons in the reconstruction of the lepton momentum can be roughly approximated by replacing m_ℓ by some scale of order Λ in the collinear logarithm.

Both Babar and Belle include sufficiently collinear photons in the definition of the lepton momentum. However, the imposed cones are so narrow that the effect for the muons is negligible, i.e. the separation of muons and collinear photons is practically perfect [10]. Thus, our expressions containing $\ln(m_b^2/m_\mu^2)$ are directly applicable in this case.

For electrons, the situation is more complicated. In both experiments, the cone is defined in the laboratory frame and has polar and azimuthal angles around 45 mrad and 5 mrad, respectively. Hence, Λ is of the same order as m_μ , which makes the QED corrections for the electrons similar to those for the muons. Nothing more precise can be said without applying dedicated Monte Carlo routines that would take into account the experimental setups in detail.

7 Formulae for the branching ratio

In Section 2, we have expressed the branching ratio in terms of the quantity $\Phi_{\ell\ell}(\hat{s})/\Phi_u$. In the present Section, we express this quantity in terms of the low-scale Wilson coefficients and various functions of \hat{s} that arise from the matrix elements. The main formula reads

$$\frac{\Phi_{\ell\ell}(\hat{s})}{\Phi_u} = \sum_{i \leq j} \text{Re} \left[C_i^{\text{eff}}(\mu_b) C_j^{\text{eff}*}(\mu_b) H_{ij}(\mu_b, \hat{s}) \right], \quad (111)$$

where $C_i^{\text{eff}}(\mu_b) \neq C_i(\mu_b)$ only for $i = 7, 8$ (see Eqs. (69) and (70)). The functions $H_{ij}(\mu_b, \hat{s})$ can be expressed analytically in terms of the coefficients M_i^A listed in Table 6 and of the following building blocks

$$\begin{aligned} S_{99} = & (1 - \hat{s})^2 (1 + 2\hat{s}) \left\{ 1 + 8 \tilde{\alpha}_s \left[\omega_{99}^{(1)}(\hat{s}) + u^{(1)} \right] + \kappa u^{(\text{em})} + 8 \tilde{\alpha}_s \kappa \omega_{99}^{(\text{em})}(\hat{s}) \right. \\ & \left. + 16 \tilde{\alpha}_s^2 \left[\omega_{99}^{(2)}(\hat{s}) + u^{(2)} + 4u^{(1)}\omega_{99}^{(1)}(\hat{s}) \right] \right\} \\ & + 6 \frac{\lambda_2}{m_b^2} (1 - 6\hat{s}^2 + 4\hat{s}^3), \end{aligned} \quad (112)$$

$$\begin{aligned} S_{77} = & (1 - \hat{s})^2 (4 + \frac{8}{\hat{s}}) \left\{ 1 + 8 \tilde{\alpha}_s \left[\omega_{77}^{(1)}(\hat{s}) + u^{(1)} \right] + \kappa u^{(\text{em})} + 8 \tilde{\alpha}_s \kappa \omega_{77}^{(\text{em})}(\hat{s}) \right\} \\ & + 24 \frac{\lambda_2}{m_b^2} (2\hat{s}^2 - 3), \end{aligned} \quad (113)$$

$$\begin{aligned} S_{79} = & 12(1 - \hat{s})^2 \left\{ 1 + 8 \tilde{\alpha}_s \left[\omega_{79}^{(1)}(\hat{s}) + u^{(1)} \right] + \kappa u^{(\text{em})} + 8 \tilde{\alpha}_s \kappa \omega_{79}^{(\text{em})}(\hat{s}) \right\} \\ & + 24 \frac{\lambda_2}{m_b^2} (1 - 6\hat{s} + 4\hat{s}^2), \end{aligned} \quad (114)$$

$$S_{1010} = S_{99} + 8 \tilde{\alpha}_s \kappa (1 - \hat{s})^2 (1 + 2\hat{s}) \left[\omega_{1010}^{(\text{em})}(\hat{s}) - \omega_{99}^{(\text{em})}(\hat{s}) \right]. \quad (115)$$

The functions $\omega_{ij}^{(k)}$ are listed in Appendix A. The functions $\omega_{ij}^{(\text{em})}$ have been given in Eqs. (94) and (100)–(105). The numbers $u^{(1)} = (4\pi^2 - 25)/12$ and $u^{(2)} \simeq 27.1 + \beta_0 u^{(1)} \ln(\mu_b/m_b)$ originate from the QCD corrections to $b \rightarrow X_u e \bar{\nu}$ [38], while the quantity $u^{(\text{em})} = \frac{12}{23}(\eta^{-1} - 1)$ stands for the logarithmically-enhanced QED correction to this decay [39]. The S_{AA} include non-perturbative $\mathcal{O}(1/m_b^2)$ corrections that one finds by taking the limit $m_c \rightarrow 0$ in Eq. (18) of Ref. [22].

The explicit expressions for the functions H_{ij} read

$$H_{ij} = \begin{cases} \sum_{A=7,9,10} |M_i^A|^2 S_{AA} + \operatorname{Re}(M_i^7 M_i^{9*}) S_{79} + \Delta H_{ii}, & \text{when } i = j \\ \sum_{A=7,9,10} 2M_i^A M_j^{A*} S_{AA} + (M_i^7 M_j^{9*} + M_i^9 M_j^{7*}) S_{79} + \Delta H_{ij}, & \text{when } i \neq j \end{cases} \quad (116)$$

It is assumed that all the products in Eq. (111) are expanded in $\tilde{\alpha}_s$, κ and λ_2 , and that higher orders are neglected (see Section 2). The quantities

$$\Delta H_{ij} = b_{ij} + c_{ij} + e_{ij} \quad (117)$$

that need to be included only for $i = 1, 2$ stand for additional bremsstrahlung (b_{ij}), non-perturbative $\mathcal{O}(1/m_c^2)$ corrections (c_{ij}) and additional $\ln(m_b^2/m_\ell^2)$ -enhanced electromagnetic corrections (e_{ij}). Specifically, the non-vanishing e_{ij} that we include read

$$\begin{aligned} e_{22} &= 8(1-\hat{s})^2(1+2\hat{s})\tilde{\alpha}_s^3\kappa^3\omega_{22}^{(\text{em})}(\hat{s}) \\ e_{27} &= 96(1-\hat{s})^2\tilde{\alpha}_s^3\kappa^3\omega_{27}^{(\text{em})}(\hat{s}) \\ e_{29} &= 8(1-\hat{s})^2(1+2\hat{s})\tilde{\alpha}_s^2\kappa^2\omega_{29}^{(\text{em})}(\hat{s}) \\ e_{11} &= \frac{16}{9}e_{22} \\ e_{12} &= \frac{8}{3}e_{22} \\ e_{1j} &= \frac{4}{3}e_{2j}, \quad \text{for } j = 7, 9. \end{aligned} \quad (118)$$

The $\mathcal{O}(1/m_c^2)$ non-perturbative contributions were calculated in Ref. [21]

$$\begin{aligned} c_{27} &= -\tilde{\alpha}_s^2\kappa^2\frac{8\lambda_2}{9m_c^2}(1-\hat{s})^2\frac{1+6\hat{s}-\hat{s}^2}{\hat{s}}\operatorname{Re}F(r), \\ c_{29} &= -\tilde{\alpha}_s\kappa\frac{8\lambda_2}{9m_c^2}(1-\hat{s})^2(2+\hat{s})\operatorname{Re}F(r), \\ c_{22} &= -\tilde{\alpha}_s\kappa\frac{8\lambda_2}{9m_c^2}(1-\hat{s})^2(2+\hat{s})\operatorname{Re}\left(F(r)M_2^{9*}\right), \\ c_{11} &= -\frac{2}{9}c_{22} \\ c_{12} &= \frac{7}{6}c_{22} \\ c_{1j} &= -\frac{1}{6}c_{2j}, \quad \text{for } j = 7, 9 \end{aligned} \quad (119)$$

where $r = 1/y_c = m_{\ell^+\ell^-}^2/(4m_c^2)$. The function $F(r)$ can be found in Appendix A.

The finite bremsstrahlung contributions b_{ij} appear at NNLO in Ref. [5], where the notation is very similar to the one proposed here. We do not present these corrections here but do include them in the numerical analysis.

8 Acknowledgments

We would like to thank Piotr Chankowski for bringing the problem of electromagnetic logarithms $\ln(M_H^2/M_L^2)$ to our attention. We are grateful to the authors of Ref. [9] for a careful reading of the manuscript and useful remarks. We are deeply indebted to Thomas Gehrmann and Aude Gehrmann-De Ridder for many discussions and help on the phase space integration. We thank Jeffrey Berryhill and Akimasa Ishikawa for information concerning the treatment of collinear photons at BaBar and Belle. This work was supported in part by the Schweizerischer Nationalfonds. M.M. acknowledges support from the Polish Committee for Scientific Research under the grant 2 P03B 078 26 and by the European Community's Human Potential Programme under the contract HPRN-CT-2002-00311, EURIDICE. Research partly supported by the Department of Energy under Grant DE-AC02-76CH03000. Fermilab is operated by Universities Research Association Inc., under contract with the U.S. Department of Energy.

A Various functions

The loop functions that appear in the text are:

$$A(x) = \frac{-3x^3 + 2x^2}{2(x-1)^4} \ln x + \frac{8x^3 + 5x^2 - 7x}{12(x-1)^3}, \quad (120)$$

$$Y(x) = \frac{3x^2}{8(x-1)^2} \ln x + \frac{x^2 - 4x}{8(x-1)}, \quad (121)$$

$$W(x) = \frac{-32x^4 + 38x^3 + 15x^2 - 18x}{18(x-1)^4} \ln x + \frac{-18x^4 + 163x^3 - 259x^2 + 108x}{36(x-1)^3}, \quad (122)$$

$$S(x) = \frac{3x^3}{2(x-1)^3} \ln x + \frac{x^3 - 11x^2 + 4x}{4(x-1)^2}, \quad (123)$$

$$X(x) = \frac{3x^2 - 6x}{8(x-1)^2} \ln x + \frac{x^2 + 2x}{8(x-1)}, \quad (124)$$

$$E(x) = \frac{x(18 - 11x - x^2)}{12(1-x)^3} + \frac{x^2(15 - 16x + 4x^2)}{6(1-x)^4} \ln x - \frac{2}{3} \ln x. \quad (125)$$

The following function appears in the matrix elements of the 4-quark operators:

$$g(y) = \frac{20}{27} + \frac{4}{9}y - \frac{2}{9}(2+y)\sqrt{|1-y|} \begin{cases} \ln \left| \frac{1+\sqrt{1-y}}{1-\sqrt{1-y}} \right| - i\pi, & \text{when } y < 1, \\ 2 \arctan \frac{1}{\sqrt{y-1}}, & \text{when } y \geq 1, \end{cases} \quad (126)$$

The $\omega_{ij}^{(n)}$ functions that include the sum of infrared divergent virtual and real contributions to the matrix elements of P_7 , P_9 and P_{10} are:

$$\omega_{99}^{(1)}(\hat{s}) = -\frac{4}{3}Li_2(\hat{s}) - \frac{2}{3} \ln(1-\hat{s}) \ln \hat{s} - \frac{2}{9}\pi^2 - \frac{5+4\hat{s}}{3(1+2\hat{s})} \ln(1-\hat{s})$$

$$-\frac{2\hat{s}(1+\hat{s})(1-2\hat{s})}{3(1-\hat{s})^2(1+2\hat{s})} \ln \hat{s} + \frac{5+9\hat{s}-6\hat{s}^2}{6(1-\hat{s})(1+2\hat{s})}, \quad (127)$$

$$\omega_{99}^{(2)}(\hat{s}) = -19.2 + 6.1\hat{s} + (37.9 + 17.2 \ln \hat{s})\hat{s}^2 - 18.7\hat{s}^3, \quad (128)$$

$$\omega_{1010}^{(1)}(\hat{s}) = \omega_{99}^{(1)}(\hat{s}), \quad (129)$$

$$\begin{aligned} \omega_{77}^{(1)}(\hat{s}) = & -\frac{4}{3}Li_2(\hat{s}) - \frac{2}{3} \ln(1-\hat{s}) \ln \hat{s} - \frac{2}{9}\pi^2 - \frac{(8+\hat{s})}{3(2+\hat{s})} \ln(1-\hat{s}) \\ & - \frac{2\hat{s}(2-2\hat{s}-\hat{s}^2)}{3(1-\hat{s})^2(2+\hat{s})} \ln \hat{s} - \frac{16-11\hat{s}-17\hat{s}^2}{18(1-\hat{s})(2+\hat{s})} - \frac{8}{3} \ln\left(\frac{\mu_b}{m_b}\right), \end{aligned} \quad (130)$$

$$\begin{aligned} \omega_{79}^{(1)}(\hat{s}) = & -\frac{4}{3}Li_2(\hat{s}) - \frac{2}{3} \ln(1-\hat{s}) \ln \hat{s} - \frac{2}{9}\pi^2 - \frac{(2+7\hat{s})}{9\hat{s}} \ln(1-\hat{s}) \\ & - \frac{2\hat{s}(3-2\hat{s})}{9(1-\hat{s})^2} \ln \hat{s} + \frac{5-9\hat{s}}{18(1-\hat{s})} - \frac{4}{3} \ln\left(\frac{\mu_b}{m_b}\right). \end{aligned} \quad (131)$$

The function $\omega_{99}^{(1)}(\hat{s})$ has been extracted [25, 26] from the $\mathcal{O}(\alpha_s)$ corrections [40] to the semileptonic decay. The functions $\omega_{77}^{(1)}(\hat{s})$ and $\omega_{79}^{(1)}(\hat{s})$ have been calculated in Ref. [4]. Note that $\omega_{77}^{(1)}(\hat{s})$ in the $\hat{s} \rightarrow 0$ limit reproduces the $\mathcal{O}(\alpha_s)$ correction [41] to the matrix element of P_7 in the $b \rightarrow X_s \gamma$ decay. The function $\omega_{99}^{(2)}(\hat{s})$ was extracted [9] from the $\mathcal{O}(\alpha_s^2)$ corrections [42, 43] to the spectrum of the $b \rightarrow X_u e \bar{\nu}$ decay. The approximate formula in Eq. (128) is valid in the range $0 < \hat{s} < 0.4$.

The function $F(r)$ that arises in the the $\mathcal{O}(1/m_c^2)$ non-perturbative corrections reads [21]

$$F(r) = \frac{3}{2r} \begin{cases} \frac{1}{\sqrt{r(1-r)}} \arctan \sqrt{\frac{r}{1-r}} - 1, & \text{when } 0 < r < 1, \\ \frac{1}{2\sqrt{r(r-1)}} \left(\ln \frac{1-\sqrt{1-1/r}}{1+\sqrt{1-1/r}} + i\pi \right) - 1, & \text{when } r > 1. \end{cases} \quad (132)$$

B \hat{V} and a_i

The numerical diagonalization of the matrix $\hat{W}^{(10)}$ yields:

$$\begin{aligned} a_i = & \left[-1.04348, -0.899395, -0.521739, -0.521739, -0.422989, 0.408619, \right. \\ & \left. 0.26087, 0.26087, 0.26087, 0.145649, 0.130435, 0, 0 \right] \quad (133) \end{aligned}$$

and

$$\hat{V} = \begin{pmatrix} 0 & 0 & 0.942522 & 0.0253179 & 0 & 0 \\ 0 & 0 & -0.314174 & -0.0084393 & 0 & 0 \\ -0.0109144 & -0.160583 & 0.0349082 & -0.0961354 & 0.917797 & -0.922049 \\ -0.0654862 & -0.984073 & -0.104725 & 0.288406 & -0.266582 & 0.331368 \\ 0.000682148 & 0.00725171 & -0.00872705 & 0.0240338 & -0.153681 & 0.130848 \\ 0.00409289 & 0.0759058 & 0.0261812 & -0.0721015 & 0.250927 & 0.151325 \\ 0 & 0 & 0 & 0 & 0 & 0 \\ 0 & 0 & 0 & 0 & 0 & 0 \\ 0.163715 & 0 & 0 & 0.291219 & 0 & 0 \\ 0.982293 & 0 & 0 & -0.873658 & 0 & 0 \\ -0.0102322 & 0 & 0 & -0.0728048 & 0 & 0 \\ -0.0613933 & 0 & 0 & 0.218414 & 0 & 0 \\ 0 & 0 & 0 & 0 & 0 & 0 \\ 0.00100213 & -0.83105 & 0.00542193 & 0 & 0 & 0 & 0 \\ 0.00066809 & -0.554033 & 0.00361462 & 0 & 0 & 0 & 0 \\ -0.0255649 & -0.0263825 & 0.0632231 & 0.726443 & 0.0531116 & 0 & 0 \\ -0.0383473 & -0.0395738 & 0.0948347 & -0.684418 & -0.0398337 & 0 & 0 \\ 0.00639122 & 0.00659563 & -0.0158058 & -0.0368909 & -0.00331947 & 0 & 0 \\ 0.00958682 & 0.00989345 & -0.0237087 & 0.0499047 & 0.00248961 & 0 & 0 \\ 0 & 0 & 0 & 0 & 0 & 1. & 0 \\ 0 & 0 & 0 & 0 & 0 & 0 & 1. \\ -0.53753 & 0 & 0 & 0 & -0.796674 & 0 & 0 \\ -0.806295 & 0 & 0 & 0 & 0.597505 & 0 & 0 \\ 0.134383 & 0 & 0 & 0 & 0.0497921 & 0 & 0 \\ 0.201574 & 0 & 0 & 0 & -0.0373441 & 0 & 0 \\ 0 & 0 & 0.993053 & 0 & 0 & 0 & 0 \end{pmatrix} \quad (134)$$

C Details of the bremsstrahlung calculation

This last appendix is devoted to some technical details of the bremsstrahlung calculation. We will integrate the sample kernel $K_R = \hat{s}_{1q}^{-1} \hat{s}_{2q}^{-1}$ over the four particle phase space, show how the Gram determinant factorizes, and explain how to extract all terms up to and including order ϵ^0 analytically. Omitting bothersome prefactors and, in addition, removing all hats from the invariants \hat{s}_{ij} we consider the expression

$$A := ds_{12} \int_0^1 ds_{1s} ds_{1q} ds_{2q} ds_{2s} ds_{sq} \delta(1 - s_{12} - s_{1s} - s_{1q} - s_{2s} - s_{2q} - s_{sq}) \times (-\Delta_4)^{-\frac{1}{2} - \epsilon} \Theta(-\Delta_4) s_{1q}^{-1} s_{2q}^{-1}, \quad (135)$$

where the Gram determinant is given by

$$\Delta_4 = (s_{12}s_{sq})^2 + (s_{1s}s_{2q})^2 + (s_{1q}s_{2s})^2 - 2(s_{12}s_{1s}s_{2q}s_{sq} + s_{1s}s_{1q}s_{2s}s_{2q} + s_{12}s_{1q}s_{2s}s_{sq}). \quad (136)$$

The first integration is over the δ -function. It is done by means of the variable s_{sq} , yielding

$$A = ds_{12} \int_0^{1-s_{12}} ds_{1s} \int_0^{1-s_{12}-s_{1s}} ds_{1q} s_{1q}^{-1} \int_0^{1-s_{12}-s_{1s}-s_{1q}} ds_{2q} s_{2q}^{-1} \int_0^{1-s_{12}-s_{1s}-s_{1q}-s_{2q}} ds_{2s} \times (-\Delta_4)^{-\frac{1}{2}-\epsilon} \Theta(-\Delta_4) \Big|_{s_{sq}=1-s_{12}-s_{1s}-s_{1q}-s_{2q}-s_{2s}}. \quad (137)$$

Substituting $s_{sq} = 1 - s_{12} - s_{1s} - s_{1q} - s_{2q} - s_{2s}$ in the Gram determinant yields an object that can be transformed into a quadratic polynomial in either of the variables s_{1s} , s_{1q} , s_{2s} or s_{2q} , *i.e.* in either variable that does not accompany s_{sq} in the quadratic piece of the Gram determinant. We choose this quadratic polynomial to be in s_{2s} :

$$-\Delta_4 = -(s_{12} + s_{1q})^2 [s_{2s}^2 + 2B s_{2s} + C] = (s_{12} + s_{1q})^2 (s_{2s}^+ - s_{2s})(s_{2s} - s_{2s}^-), \quad (138)$$

where s_{2s}^\pm are the roots of the quadratic polynomial:

$$s_{2s}^\pm = -B \pm \sqrt{B^2 - C} \equiv -B \pm \sqrt{\Xi}. \quad (139)$$

The Θ -function now requires these roots to be real** which is equivalent to the condition $\Xi \geq 0$. From the latter inequality we conclude

$$s_{2q} \leq z(1 - s_{12} - s_{1s} - s_{1q}) \quad \text{with} \quad z = \frac{s_{12} + s_{1q}}{s_{12} + s_{1q} + s_{1s}} \leq 1 \quad (140)$$

The above roots now fulfill the inequality $0 \leq s_{2s}^- \leq s_{2s}^+ \leq 1 - s_{12} - s_{1s} - s_{1q} - s_{2q}$ which leads to the following new limits of integration:

$$A = ds_{12} \int_0^{1-s_{12}} ds_{1s} \int_0^{1-s_{12}-s_{1s}} ds_{1q} s_{1q}^{-1} (s_{12} + s_{1q})^{-1-2\epsilon} \times \int_0^{z(1-s_{12}-s_{1s}-s_{1q})} ds_{2q} s_{2q}^{-1} \int_{s_{2s}^-}^{s_{2s}^+} ds_{2s} (s_{2s}^+ - s_{2s})^{-\frac{1}{2}-\epsilon} (s_{2s} - s_{2s}^-)^{-\frac{1}{2}-\epsilon}. \quad (141)$$

Substituting $s_{2s} = (s_{2s}^+ - s_{2s}^-)\chi + s_{2s}^-$, the subsequent χ -integration can be done trivially in terms of Γ -functions.

As a general strategy for the choice of the order of integration, we suggest the following. The variable of the first integration (δ -function) must not be contained in the term of K_R that one considers. If possible, this term should also be free of the variable that one uses to factorize the Gram determinant (s_{2s} in our case). If the latter is not possible as for instance in $K_R = s_{1s} s_{2s} s_{1q}^{-1} s_{2q}^{-1}$, one should at least factorize the Gram determinant in a variable that does not appear in the denominator of K_R . This procedure ensures that the first two integrations can be done in terms of Γ -functions, and it avoids hypergeometric functions to emerge at this stage of the calculation.

**otherwise $-\Delta_4$ is negative for all s_{2s}

The choice of the subsequent order of integration is governed by the aim to extract all divergences as early as possible, this being the reason why we solved the condition $\Xi \geq 0$ for s_{2q} . We now substitute $s_{2q} = z(1 - s_{12} - s_{1s} - s_{1q})t$ and perform the t -integration, yielding again only Γ -functions. After simplification, we obtain

$$A = -\frac{\pi}{\epsilon} ds_{12} s_{12}^{-\epsilon} \int_0^{1-s_{12}} ds_{1s} s_{1s}^{-\epsilon} \int_0^{1-s_{12}-s_{1s}} ds_{1q} s_{1q}^{-1-\epsilon} (s_{12} + s_{1q})^{-1} (s_{12} + s_{1q} + s_{1s})^\epsilon (1 - s_{12} - s_{1s} - s_{1q})^{-2\epsilon}. \quad (142)$$

We now proceed as follows

- Perform an expansion into partial fractions via $\frac{1}{s_{1q}(s_{12} + s_{1q})} = \frac{1}{s_{12}s_{1q}} - \frac{1}{s_{12}(s_{12} + s_{1q})}$
- Substitute $s_{1q} = (1 - s_{12} - s_{1s})(1 - u)$. The u -integration can be carried out in the first term of the above expansion.
- Substitute $s_{1s} = (1 - s_{12})(1 - v)$, again the v -integration can be done in the first term.

One now obtains the following expression:

$$A = -\frac{\pi}{\epsilon} ds_{12} s_{12}^{-1-\epsilon} (1 - s_{12})^{1-4\epsilon} \left\{ \frac{\Gamma(1-2\epsilon)\Gamma(-\epsilon)\Gamma(1-\epsilon)}{\Gamma(2-4\epsilon)} {}_2F_1(-\epsilon, 1-2\epsilon; 2-4\epsilon; 1-s_{12}) \right. \\ \left. - (1-s_{12}) \int_0^1 du \int_0^1 dv \frac{u^{-2\epsilon}(1-u)^{-\epsilon} v^{1-3\epsilon}(1-v)^{-\epsilon}}{s_{12} + (1-s_{12})v(1-u)} [1 - (1-s_{12})uv]^\epsilon \right\}. \quad (143)$$

We now carry out a two-dimensional variable transformation from (u, v) to (y, w) via

$$y = 1 - uv \quad \text{and} \quad yw = v(1-u). \quad (144)$$

The w -integration can now be performed, resulting in another hypergeometric function. After using the Kummer relation, also the y -integration can be done. The final result for A reads

$$A = -\frac{\pi}{\epsilon} ds_{12} s_{12}^{-1-\epsilon} (1 - s_{12})^{1-4\epsilon} \left\{ \frac{\Gamma(1-2\epsilon)\Gamma(-\epsilon)\Gamma(1-\epsilon)}{\Gamma(2-4\epsilon)} {}_2F_1(-\epsilon, 1-2\epsilon; 2-4\epsilon; 1-s_{12}) \right. \\ \left. - (1-s_{12}) \frac{\Gamma^2(1-\epsilon)\Gamma(1-2\epsilon)}{\Gamma(3-4\epsilon)} {}_2F_1(1-\epsilon, 2-2\epsilon; 3-4\epsilon; 1-s_{12}) \right\}. \quad (145)$$

All the divergences have now been extracted in terms of poles and Γ -functions. The remaining task is now to expand the hypergeometric functions in ϵ . This can be done by means of the **Mathematica** package **HypExp** [44].

References

- [1] M. Iwasaki *et al.* [Belle Collaboration], hep-ex/0503044.
- [2] B. Aubert *et al.* [BABAR Collaboration], Phys. Rev. Lett. **93** (2004) 081802 [hep-ex/0404006].
- [3] C. Bobeth, M. Misiak and J. Urban, Nucl. Phys. B **574** (2000) 291 [hep-ph/9910220].
- [4] H. H. Asatryan, H. M. Asatrian, C. Greub and M. Walker, Phys. Rev. D **65** (2002) 074004 [hep-ph/0109140].
- [5] H. H. Asatryan, H. M. Asatrian, C. Greub and M. Walker, Phys. Rev. D **66** (2002) 034009 [hep-ph/0204341].
- [6] A. Ghinculov, T. Hurth, G. Isidori and Y. P. Yao, Nucl. Phys. B **685**, 351 (2004) [hep-ph/0312128].
- [7] P. Gambino, M. Gorbahn and U. Haisch, Nucl. Phys. B **673** (2003) 238 [hep-ph/0306079].
- [8] M. Gorbahn and U. Haisch, Nucl. Phys. B **713** (2005) 291 [hep-ph/0411071].
- [9] C. Bobeth, P. Gambino, M. Gorbahn and U. Haisch, JHEP **0404** (2004) 071 [hep-ph/0312090].
- [10] J. Berryhill, A. Ishikawa, private communication.
- [11] P. Gambino and M. Misiak, Nucl. Phys. B **611**, 338 (2001) [hep-ph/0104034].
- [12] C. W. Bauer, Z. Ligeti, M. Luke, A. V. Manohar and M. Trott, Phys. Rev. D **70**, 094017 (2004) [hep-ph/0408002].
- [13] S. Bethke, Nucl. Phys. Proc. Suppl. **135**, 345 (2004) [hep-ex/0407021].
- [14] J. Charles *et al.* [CKMfitter Group], Eur. Phys. J. C **41**, 1 (2005) [hep-ph/0406184].
- [15] A. H. Hoang and A. V. Manohar, hep-ph/0509195.
- [16] B. Aubert *et al.* (BaBar Collaboration), Phys. Rev. Lett. **93**, 011803 (2004) [hep-ex/0404017].
- [17] [CDF Collaboration], hep-ex/0507091.
- [18] S. Eidelman *et al.* [Particle Data Group], Phys. Lett. B **592**, 1 (2004).
- [19] A. H. Hoang, Z. Ligeti and A. V. Manohar, Phys. Rev. D **59** (1999) 074017 [hep-ph/9811239].
- [20] A. H. Hoang, hep-ph/0008102.

- [21] G. Buchalla, G. Isidori and S. J. Rey, Nucl. Phys. B **511** (1998) 594 [hep-ph/9705253].
- [22] G. Buchalla and G. Isidori, Nucl. Phys. B **525**, 333 (1998) [hep-ph/9801456].
- [23] A.F. Falk, M.E. Luke and M.J. Savage, Phys. Rev. D **49** (1994) 3367 [hep-ph/9308288]; A. Ali, G. Hiller, L. T. Handoko and T. Morozumi, Phys. Rev. D **55**, 4105 (1997) [hep-ph/9609449].
- [24] A. J. Buras, hep-ph/9806471.
- [25] M. Misiak, Nucl. Phys. B **393** (1993) 23 [Erratum-ibid. B **439** (1995) 461].
- [26] A. J. Buras and M. Münz, Phys. Rev. D **52** (1995) 186 [hep-ph/9501281].
- [27] P. Gambino and U. Haisch, JHEP **0110** (2001) 020 [hep-ph/0109058].
- [28] G. Buchalla, A. J. Buras and M. K. Harlander, Nucl. Phys. B **337** (1990) 313.
- [29] G. Buchalla and A. J. Buras, Phys. Rev. D **57** (1998) 216 [hep-ph/9707243].
- [30] A. J. Buras, P. Gambino and U. A. Haisch, Nucl. Phys. B **570** (2000) 117 [hep-ph/9911250].
- [31] T. van Ritbergen, J. A. M. Vermaseren and S. A. Larin, Phys. Lett. B **400** (1997) 379 [hep-ph/9701390].
- [32] M. Czakon, Nucl. Phys. B **710**, 485 (2005) [hep-ph/0411261].
- [33] K.G. Chetyrkin, M. Misiak and M. Münz, Phys. Lett. B **400** (1997) 206, Phys. Lett. B **425** (1998) 414 (E) [hep-ph/9612313].
- [34] K. Baranowski and M. Misiak, Phys. Lett. B **483** (2000) 410 [hep-ph/9907427].
- [35] A. Gehrman-De Ridder, T. Gehrman and G. Heinrich, Nucl. Phys. B **682** (2004) 265 [hep-ph/0311276].
- [36] H. Terazawa, Rev. Mod. Phys. **45** (1973) 615.
- [37] B. Mele and P. Nason, Nucl. Phys. B **361**, 626 (1991).
- [38] T. van Ritbergen, Phys. Lett. B **454** (1999) 353 [hep-ph/9903226].
- [39] A. Sirlin, Nucl. Phys. B **196** (1982) 83.
- [40] M. Jeżabek and J. H. Kühn, Nucl. Phys. B **320** (1989) 20.
- [41] A. Ali and C. Greub, Z. Phys. C **49** (1991) 431, Phys. Lett. B **259** (1991) 182, Phys. Lett. B **361** (1995) 146 [hep-ph/9506374].
- [42] K. G. Chetyrkin, R. Harlander, T. Seidensticker and M. Steinhauser, Phys. Rev. D **60** (1999) 114015 [hep-ph/9906273].

- [43] A. Czarnecki and K. Melnikov, Phys. Rev. Lett. **88** (2002) 131801 [arXiv:hep-ph/0112264].
- [44] T. Huber and D. Maitre, hep-ph/0507094.